Supporting Information

Enantioselective Synthesis of Pharmaceutically Active γ-Aminobutyric Acids Using a Tailor-Made Artificial Michaelase in One-Pot Cascade Reactions

Lieuwe Biewenga[†a], Thangavelu Saravanan[†a], Andreas Kunzendorf[a], Jan-Ytzen van der Meer[a], Tjaard Pijning[b], Pieter G. Tepper[a], Ronald van Merkerk[a], Simon J. Charnock[c], Andy-Mark W. H. Thunnissen[d], and Gerrit J. Poelarends*[a]

[a]Department of Chemical and Pharmaceutical Biology, Groningen Research Institute of Pharmacy, University of Groningen, Antonius Deusinglaan 1, 9713 AV Groningen, The Netherlands.

[b]Structural Biology Group, Groningen Institute of Biomolecular Sciences and Biotechnology, University of Groningen, Nijenborgh 7, 9747 AG Groningen, The Netherlands.

[c]Prozomix Ltd., Station Court, Haltwhistle, Northumberland NE49 9HN, U.K.

[d]Molecular Enzymology Group, Groningen Institute of Biomolecular Sciences and Biotechnology, University of Groningen, Nijenborgh 7, 9747 AG Groningen, The Netherlands.

[†]These authors contributed equally: Lieuwe Biewenga and Thangavelu Saravanan.

*Corresponding author. Tel.: +31503633354; E-mail: g.j.poelarends@rug.nl; Web: http://www.rug.nl/staff/g.j.poelarends/

Table of contents

Supporting methods

Mutant library construction

The 4-OT I2X/L8X/M45Y/F50A library was constructed by Quikchange mutagenesis. The following primers were used: Fw 5'-GGA GAT ATA CAT ATG CCT **NNK** GCC CAG ATC CAC ATC **NNK** GAA GGC CGC AGC G-3' and Rv 5'-C GCT GCG GCC TTC **MNN** GAT GTG GAT CTG GGC **MNN** AGG CAT ATG TAT ATC TCC-3'. The mutated codons are indicated in bold. An amount of 40 ng of pJexpress 414 plasmid DNA containing the 4-OT M45Y/F50A gene was used as template[1]. The PCR reaction was conducted using Phusion polymerase (New England Biolabs) in 1x HF buffer (New England Biolabs) in 50 µl reaction volume. The following PCR program was used: 98 °C, 10 min (initial denaturation), followed by 18 cycles of 95 °C for 30 s, 55 °C for 1 min, 68 °C for 4 min and a final elongation step of 68 °C for 10 min. The reaction mixtures were 2x diluted with water followed by the addition of 1 µl FastDigest DpnI (ThermoFisher Scientific) to digest the template DNA. Reaction mixtures were placed at 37 °C for 2 h, followed by a DpnI denaturing step of 80 °C for 10 min. An initial transformation in *Escherichia coli* Dh5α cells was performed and the plasmid DNA of individual colonies was isolated and sequenced to confirm the library quality. To collect the library DNA, four parallel transformations were performed using 50 µl of 10-beta competent *E. coli* cells (High efficiency, New England Biolabs) and 5 µl of the PCR reaction mixture. Transformants were selected on LB-agar plates supplemented with 100 µg/ml ampicillin. About 8000 colonies were resuspended in 10 mM sodium phosphate buffer and plasmid DNA was isolated and subsequently used to transform *E. coli* BL21(DE3) cells for expression of the 4-OT mutants.

Production and purification of enzymes

The enzyme 4-OT M45Y/F50A was purified according to an earlier described purification procedure[2]. Mutant enzymes 4-OT I2M/L8Y/M45Y/F50A, 4-OT I2W/L8Y/M45Y/F50A, 4-OT L8F/M45Y/F50A and 4-OT L8Y/M45Y/F50A were purified according to a modified protocol. Accordingly, the cell pellets were resuspended in 10 mM TRIS buffer pH 8 (instead of 10 mM sodium phosphate buffer). After loading on the DEAE-sepharose column, the column was washed 2x with 8 ml 10 mM TRIS buffer pH 8. The 4-

OT enzyme was eluted with 3x 8 ml of 10 mM sodium phosphate buffer pH 7.3. Typically, the second and third elution fraction would contain pure 4-OT (>95% purity as determined by SDS-PAGE). Fractions containing pure 4-OT enzyme were combined and concentrated using a vivaspin centrifugal concentrator (Sartorius, 5000 MWCO). After concentration to ~3 ml, the sample was two times diafiltrated with 20 ml of 10 mM sodium phosphate buffer pH 7.3 to remove any traces of the TRIS buffer. The concentration of purified 4-OT was determined by the Waddell method[3]. The purified 4-OT was aliquoted, flash frozen in liquid nitrogen and stored at -80 °C until further use. All purified 4-OT mutants were analyzed by electron spray ionization mass spectrometry to confirm the correct mass of the protein. PRO-ALDH(003) and PRO-NOX(009) were provided as crude cell-free extracts by Prozomix Ltd, and used without any further purification.

Progress curves of the enzyme-catalyzed reactions

To monitor the progress of the enzymatic addition of **1** to **2a**, the reaction mixtures consisted of the following: 5 mM **2a**, DMSO (5% v/v), 100 µM 4-OT (2 mol% compared to **2a**) in 20 mM sodium phosphate buffer pH 6.5, 500 µl final volume. The reaction was initiated by the addition of **1** to a final concentration of 150 mM (from a freshly prepared 1.5 M stock solution in 20 mM sodium phosphate buffer pH 6.5). Every 8 min a sample was withdrawn from the reaction mixture and a UV-VIS spectrum was measured from 200 to 500 nm. After the measurement, the sample was returned to the reaction mixture. The progress curve was constructed based on the depletion in absorbance at 249 nm, which corresponds to the λ_{max} of substrate **2a**[4]. After 88 minutes, the reaction mixtures were extracted with 500 µl toluene. The organic layer was separated from the aqueous layer by centrifugation. A sample from the organic layer was transferred to a GC vial and analyzed by GC with a chiral stationary phase (see library screening). No product **3a** could be identified for the control reaction without enzyme.

To monitor the progress of the enzymatic addition of **1** to **2c**, the reaction mixtures consisted of the following: 1.3 mM **2c**, DMSO (45% v/v), 18 µM 4-OT (1.4 mol% compared to **2c**) in 20 mM sodium phosphate buffer pH 6.5, 500 µl final volume. The reaction was initiated by the addition of **1** to a final concentration of 65 mM (from a freshly prepared 650 mM stock solution in sodium phosphate buffer

pH 6.5). Every 8 min a sample was withdrawn from the reaction mixture and a UV-VIS spectrum was measured from 200 to 500 nm. After the measurement, the sample was returned to the reaction mixture. The progress curve was constructed based on the depletion in absorbance at 320 nm, which corresponds to the λ_{max} of substrate **2c**[4].

Crystallization and data collection

The newly engineered artificial Michaelase (4-OT L8Y/M45Y/F50A) was crystallized by hanging drop vapour diffusion at 293 K. Drops consisted of equal volumes of protein solution (14.5 mg/ml) in 10 mM sodium phosphate buffer, pH 7.3 and 18% (w/v) PEG 3350, 0.2 M sodium formate, 0.1 M Bis-Tris propane-HCl, pH 7.0. Rod-like crystals appeared within a few days and were cryoprotected using 24% (w/v) PEG 3350, 16% (v/v) glycerol, 50 mM sodium formate, 50 mM Bis-Tris propane-HCl, pH 6.5. Diffraction data were collected at beamline P11 of DESY (Hamburg, Germany) and indexed, integrated and scaled using XDS[5]. Statistics are given in Table S2.

Structure determination and refinement

The structure of 4-OT L8Y/M45Y/F50A, containing three hexamers (chains A-F, G-L and M-R) in the asymmetric unit of the *P* $2_12_12_1$ cell, was determined by molecular replacement using PHASER[6] with the wild-type 4-OT structure (PDB entry: 4X19)[7] as a search model. Crystallographic refinement was carried out with Refmac[8] using non-crystallographic symmetry restraints, and alternated with map inspection and manual rebuilding in Coot[9]. Refinement statistics and model quality are given in Table S2. Structural figures were prepared with PyMOL (The PyMOL Molecular Graphics System, Version 2.0 Schrödinger, LLC). Atomic coordinates and structure factors have been deposited at the Protein Data Bank with entry 6FPS.

Solvent screening

The effect of increasing concentrations of different co-solvents on the enantioselectivity of 4-OT M45Y/F50A for the addition of **1** to **2a** was investigated. Small scale reactions were set up consisting

of the following: 325 µg 4-OT M45Y/F50A (160 µM), 3 mM **2a**, 50 mM **1**, and co-solvent in 20 mM sodium phosphate buffer pH 5.5, 300 µl final volume. The reactions were performed in a 1 mm quartz cuvette. The following co-solvents were used: DMSO, ethanol, methanol, isobutanol, PEG400, 1,4-butanediol, 1,3-propanediol, ethylene glycol, glyceline, and ethaline in concentrations ranging from 1% to 70%. The decrease in absorbance at 249 nm, corresponding to the concentration of **2a**, was followed over time. In case 4-OT M45Y/F50A precipitated during the course of the reaction, the reaction mixture was discarded. After the reaction was finished, the reaction mixture was extracted with 700 µl toluene. The organic layer was collected and concentrated by applying a N_2 flow. A sample of the remaining organic layer was analyzed by GC to determine the enantiopurity of the enzymatic product **3a**. The following GC program was used: gradual temperature increase: 40 °C to 120 °C at 10 °C per min. Gradual temperature increase 120 °C to 140 °C at 0.5 °C per min. Gradual temperature decrease 140 °C to 40 °C at 10 °C per min. Flame ionization detection: Retention time *S*-enantiomer: 30.4 min, retention time *R*-enantiomer 31.3 min. The assignment of the absolute configuration was based on earlier reported data[1,4].

Synthesis of racemic references

Synthesis of racemic γ-nitrobutyraldehydes

The racemic γ-nitrobutyraldehydes **3a-d**, which served as reference compounds for analyses by HPLC and GC on a chiral stationary phase, were synthesized according to literature procedures[4].

Synthesis of racemic γ-nitrobutyric acids (4a-d)

The racemic γ-nitrobutyric acids **4a-d** were synthesized from the corresponding racemic γ-nitrobutyraldehydes **3a-d** according to literature procedures[10]. The racemic γ-nitrobutraldehyde **3a** (0.5 mmol) was dissolved in 3 ml of *tert*-butanol:water (3:1) and cooled to 0°C. To this $NaH_2PO_4 \cdot 2H_2O$ (1 mmol), 2-methyl-2-butene (2 mmol) and $NaClO_2$ (6.96 g, 1.5 mmol) were added and the mixture was stirred for 30 min. The reaction mixture was quenched with a saturated NH_4Cl solution and extracted with EtOAc. The organic layer was dried over anhydrous $MgSO_4$, concentrated in vacuo and the crude reaction product was purified by silica gel column chromatography using petroleum ether:EtOAc (8:2) to get racemic **4a**. The same procedure was followed for the synthesis of **4b- 4d**.

Synthesis of racemic γ-aminobutyric acids (5a-d)

Racemic γ-aminobutyric acids **5a** and **5c** were commercially available. Racemic **5b** and **5d** were synthesized from the corresponding racemic γ-nitrobutyric acids (**4b** and **4d**) according to literature procedures[11]. Racemic **4b** (0.1 mmol) was dissolved in 10% ethanol (3 ml) and cooled to 0°C. To this $NiCl_2 \cdot 6H_2O$ (1 mmol), followed by $NaBH_4$ (1 mmol) was added carefully. The reaction mixture was stirred at room temperature for 24 h. After complete conversion, the reaction mixture was filtered through celite pad and the filtrate was concentrated in vacuo. The resulting concentrated mixture was acidified to pH 3-4 and then loaded on a column packed with cation exchange resin (5 g of Dowex® 50WX8 hydrogen form). After washing with deionized water (4 column volumes), the product was eluted out with 0.5 M (4 column volumes) - 1 M ammonia solution (4 column volumes). The ninhydrin-positive fractions were collected, combined and lyophilized to yield racemic product **5b**. Racemic **5d** was synthesized by following the same procedure.

Product derivatization for determination of enantiomeric excess and reaction progress

Derivatization of 3b and 3c for enantiomeric excess determination

The aldehyde functionality of **3b** was derivatized to a cyclic acetal according to a literature procedure[4,12]. The aldehyde functionality of **3c** was also derivatized to the cyclic acetal. To a solution of 100 mg (0.44 mmol) racemic **3c** in 16 ml DCM (anhydrous) and 0.51 g (8.2 mmol) ethylene glycol (anhydrous), 15 mg of paratoluene sulfonic acid was added. The reaction was stirred overnight at room temperature. After silica column purification the cyclic acetal was obtained (91 mg, 76% yield).

^{1}H NMR (500 MHz, Chloroform-*d*) δ 7.30 (d, *J* = 8.4 Hz, 2H), 7.17 (d, *J* = 8.5 Hz, 2H), 4.76 (dd, *J* = 12.7, 6.1 Hz, 1H), 4.73 (dd, *J* = 6.2, 3.2 Hz, 0H), 4.55 (dd, *J* = 12.6, 9.4 Hz, 1H), 3.99 – 3.93 (m, 1H), 3.85 – 3.79 (m, 1H), 3.79 – 3.72 (m, 1H), 2.08 (ddd, *J* = 14.2, 7.7, 3.2 Hz, 1H), 2.00 – 1.94 (m, 1H).

^{13}C NMR (126 MHz, $CDCl_3$) δ 137.97, 133.68, 129.30, 128.93, 102.21, 80.26, 65.12, 65.05, 39.43, 37.27.

Derivatization for HPLC analysis of reaction progress[13]

For the cascade reactions, a sample (50 µl) from the reaction mixture was taken at constant time intervals and mixed with 50 µL of derivatizing agent, which contains O-benzylhydroxylamine hydrochloride 40 mg mL^{-1}; 0.25 mmol mL^{-1} in pyridine:methanol:water (9:9:2). After incubation for 30 min at room temperature, the sample was centrifuged at 13,000 rpm for 10 min and then the

supernatant was analyzed by reverse phase HPLC using a C18 column (Kinetex 5u EVO C18 100A, 150 mm x 4.6 mm, Phenomenex®). Mobile phase A was water with 0.1% TFA and mobile phase B was ACN with 0.1% TFA. The detailed mobile phase gradient was as follows: 0 min, 5% B; 0.01–6 min, 8-35% B; 6–14 min, 35–85% B; 14–15.5 min, 85–90% B; 15.5–16.5 min 90–8% B and 16.5–20 min, 5% B, while the flow rate was 1 ml/min.

Derivatization of 4a-d for enantiomeric excess determination

The compound **4a** (0.1 mmol) was dissolved in dichloromethane (1 ml) and methanol (0.2 ml), and cooled down to 0 °C. To this cooled solution, EDC.HCl (0.15 mmol) was added, followed by DMAP (0.01 mmol). After 1 h, the reaction mixture was quenched with saturated NH_4Cl, extracted with diethyl ether and the organic layer was dried over anhydrous Na_2SO_4. The dried organic layer was concentrated in vacuo and the crude product was purified by silica gel column chromatography (hexane/ethylacetate 9:1) to yield the methyl ester of **4a** (75% yield). The same procedure was followed for derivatization of **4b-d**.

Derivatization of 5a-d for enantiomeric excess determination

γ-Aminobutyric acids **5a-d** were derivatized to diastereomers using sodium 2,4-dinitro-5-fluorophenyl-L-valine amide[14]. To a solution of **5a** in water (0.1 ml, 1 mg/ml), a freshly prepared solution of sodium 2,4-dinitro-5-fluorophenyl-L-valine amide in MeCN/water 10:90 (0.1 ml, 10 mg/ml) was added. To this triethylamine (2.5 µl) was added and the sample was vortexed at high speed. After 10 min incubation at room temperature, the sample was directly analyzed by HPLC. The same procedure was followed for derivatization of **5b-d**.

Supporting Tables

Table S1. Enantioselectivity of 4-OT mutants for the addition of **1** to **2a** to yield **3a**[a].

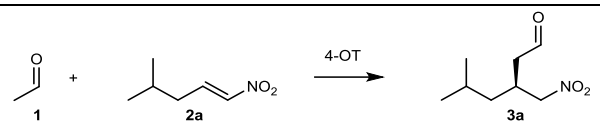

1 2a 3a

Entry	4-OT mutant	Co-solvent	Product e.r.[b]	Abs. Conf.[c]
1	M45Y/F50A	5 % DMSO	90:10	*S*
2	I2W/L8Y/M45Y/F50A	5 % DMSO	99:1	*S*
3	I2M/L8Y/M45Y/F50A	5 % DMSO	99:1	*S*
4	L8F/M45Y/F50A	5 % DMSO	99:1	*S*
5	L8Y/M45Y/F50A	5 % DMSO	99:1	*S*
6	L8Y/M45Y/F50A	25 % EtOH	>99:1	*S*

[a] Assay conditions: The reaction mixture consisted of 150 mM **1**, 5 mM **2a**, and 100 µM of biocatalyst in 20 mM sodium phosphate buffer pH 6.5, 300 µl reaction volume.

[b] Determined by GC with a chiral stationary phase.

[c] Determined by literature comparison[1,4].

Table S2. Crystallographic data.

PDB entry	6FPS
Data collection	
Space group	$P\ 2_12_12_1$
Cell dimensions *a*, *b*, *c* (Å)	90.0, 99.5, 118.3
Resolution (Å)	46-1.90 (1.93-1.90)
R_{merge}	0.081 (1.43)
R_{pim}	0.044 (0.820)
$CC_{1/2}$	0.999 (0.742)
$< I/\sigma >$	14.2 (1.5)
Completeness (%) *	100.0 (100.0)
Redundancy *	8.1(7.7)
Refinement	
Resolution (Å)	46-1.90 (1.93-1.90)
Unique observations *	80195 (4096)
R / R_{free}	0.201 / 0.222
Number of atoms	
protein	8283
waters	341
Ligand molecules	phosphate ion (1), glycerol (1)
Average B-factor protein ($Å^2$)	39.3
Root mean square deviations	
Bond lengths (Å)	0.015
Bond angles (^{o})	1.64
Ramachandran	
Favored (%)	99.9
Allowed (%)	0.1
Outliers (%)	0.0

* values in brackets refer to the highest resolution shell

Supporting Figures

GC chromatograms of products from small scale reactions

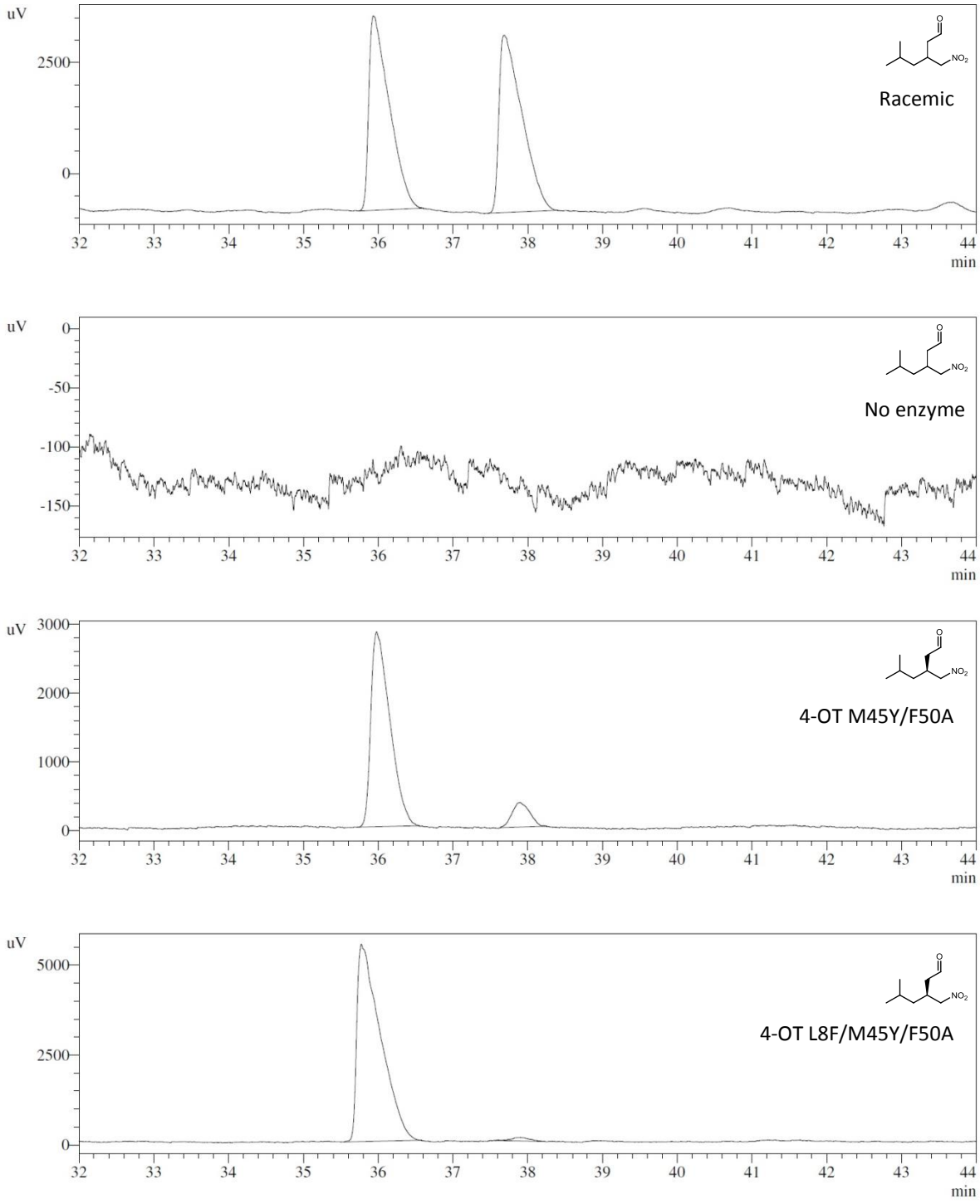

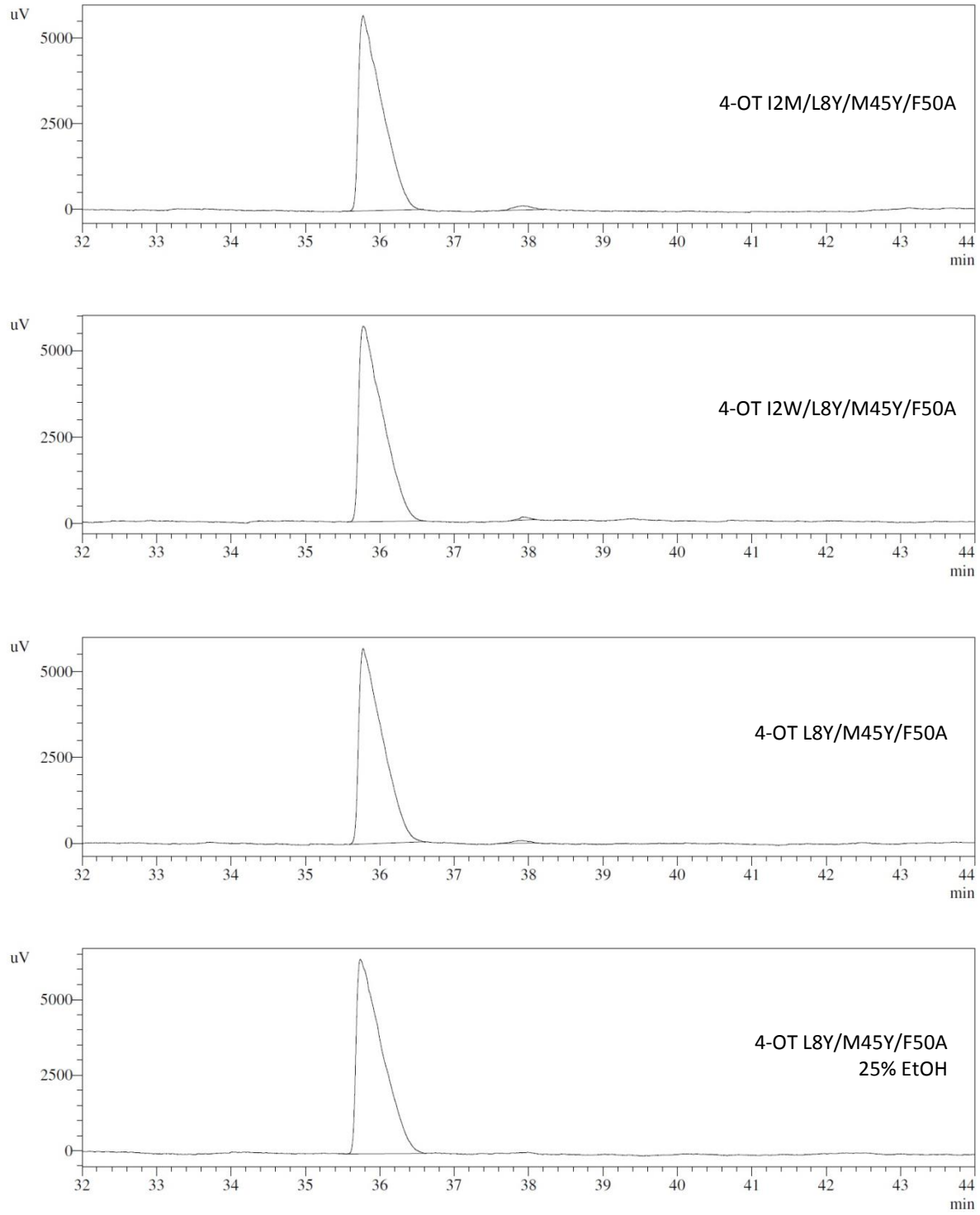

Figure S1. GC chromatograms of racemic or enzymatically obtained **3a** in small scale reactions. The experimental conditions and product e.r. values are listed in Table S1.

UV absorbance spectra monitoring the 4-OT L8Y/M45Y/F50A catalyzed addition of 1 to 2a-d

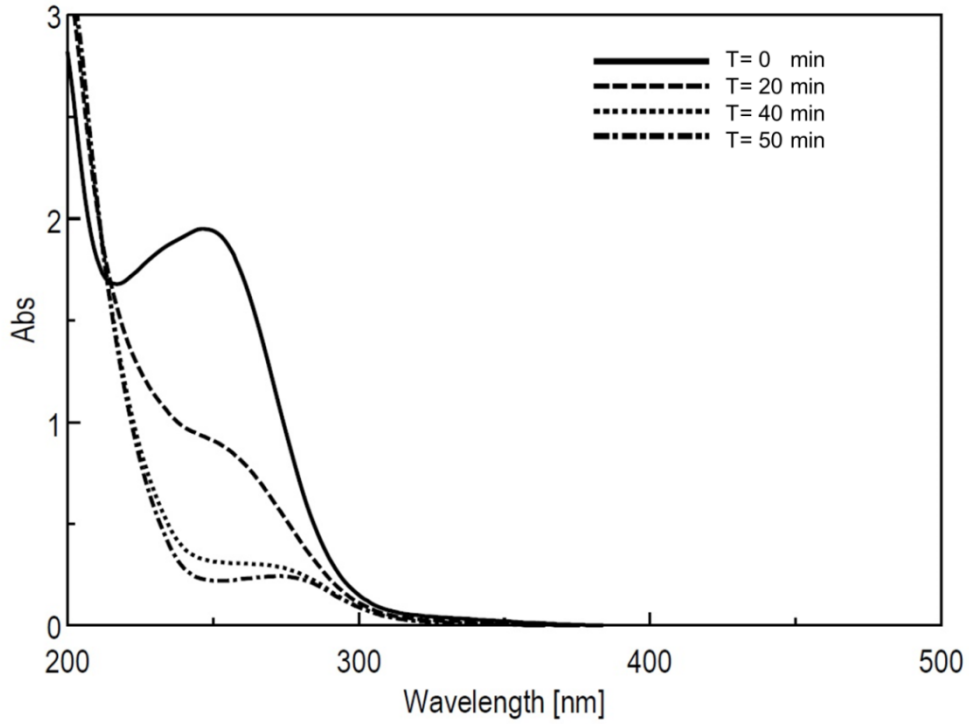

Figure S2. UV spectra showing the conversion of **2a** catalyzed by 4-OT L8Y/M45Y/F50A in 20 mM sodium phosphate buffer, pH 6.5, 20% ethanol.

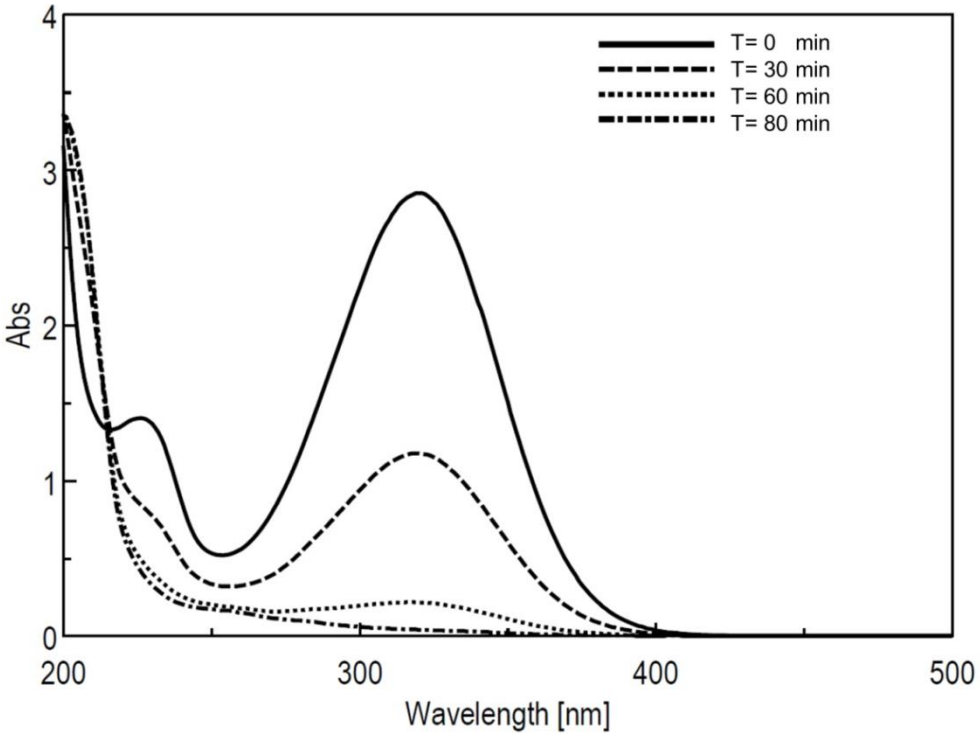

Figure S3. UV spectra showing the conversion of **2b** catalyzed by 4-OT L8Y/M45Y/F50A in 20 mM sodium phosphate buffer, pH 6.5, 20% ethanol.

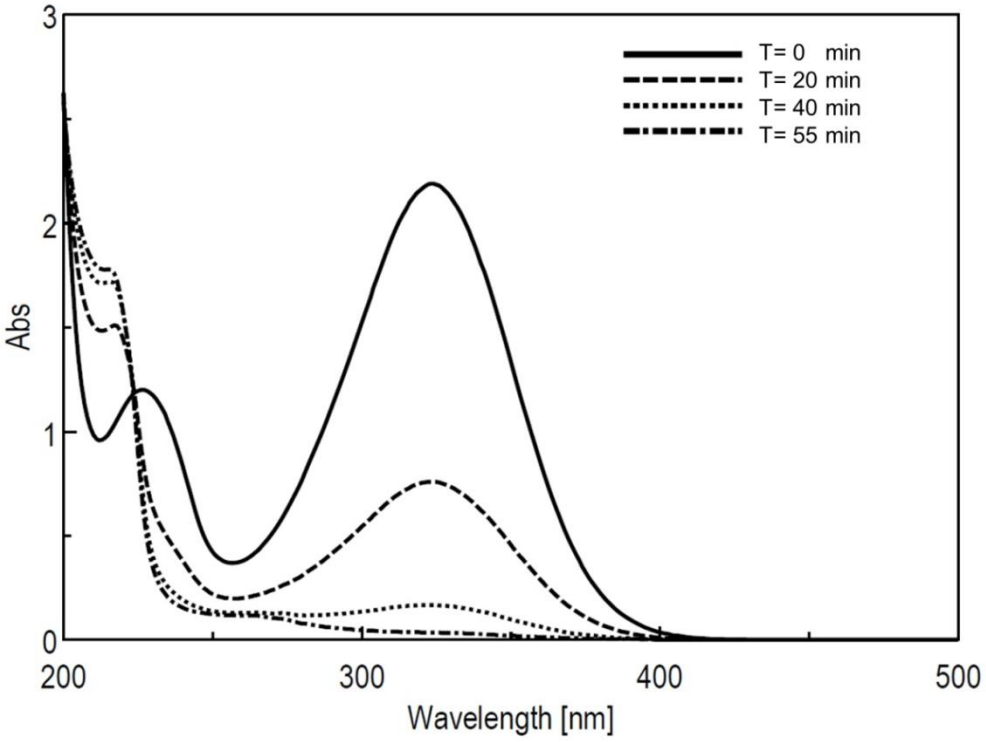

Figure S4. UV spectra showing the conversion of **2c** catalyzed by 4-OT L8Y/M45Y/F50A in 20 mM sodium phosphate buffer, pH 6.5, 30% ethanol.

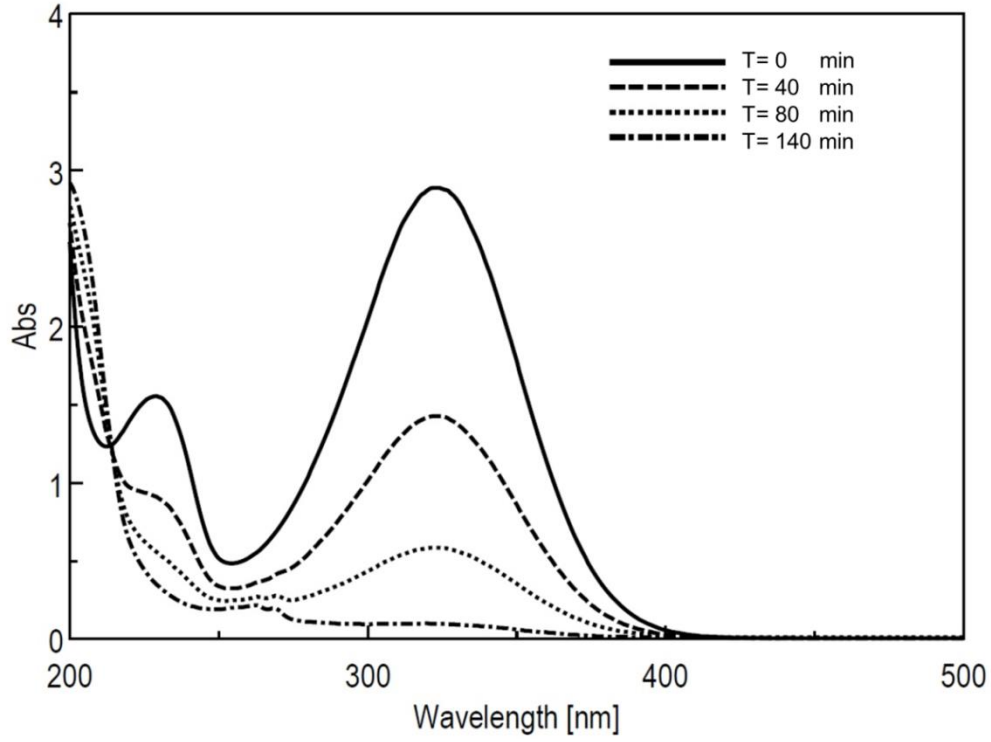

Figure S5. UV spectra showing the conversion of **2d** catalyzed by 4-OT L8Y/M45Y/F50A in 20 mM sodium phosphate buffer, pH 6.5, 20% ethanol.

^{1}H NMR spectra of enzymatically obtained 3a-d

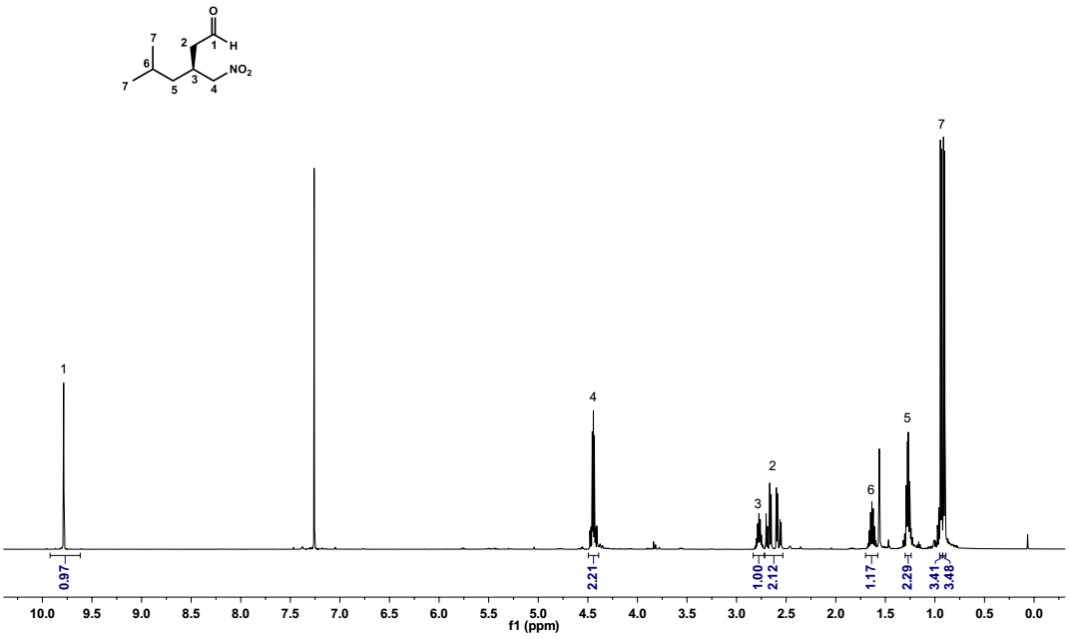

Figure S6. ^{1}H NMR spectrum of enzymatically prepared (*S*)-5-methyl-3-(nitromethyl)hexanal (**3a**) (400 MHz, $CDCl_3$).

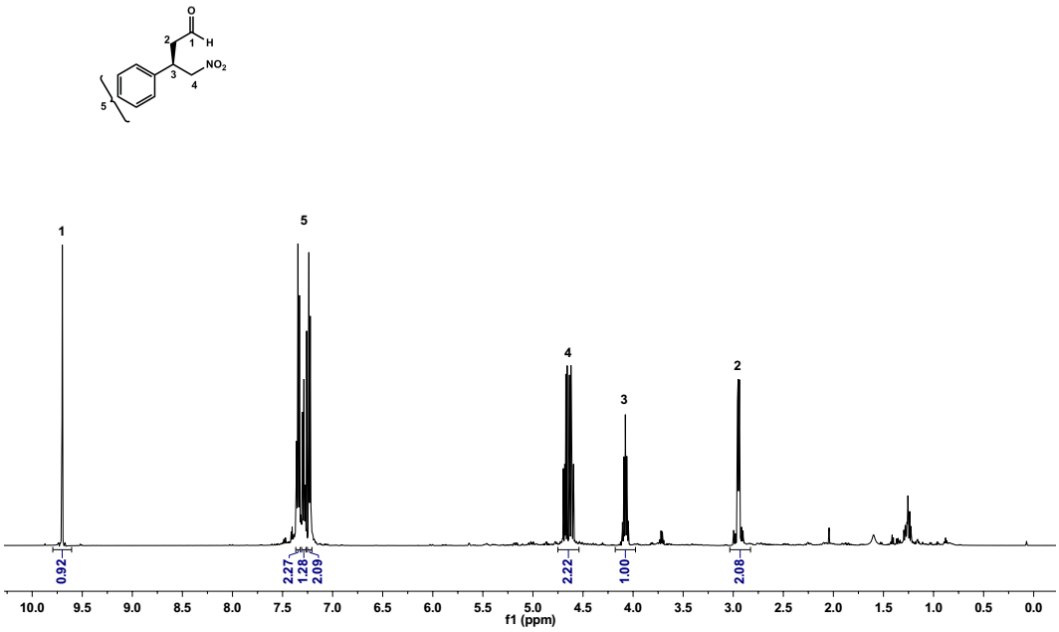

Figure S7. ^{1}H NMR spectrum of enzymatically prepared (*R*)-4-nitro-3-phenylbutanal (**3b**) (400 MHz, $CDCl_3$).

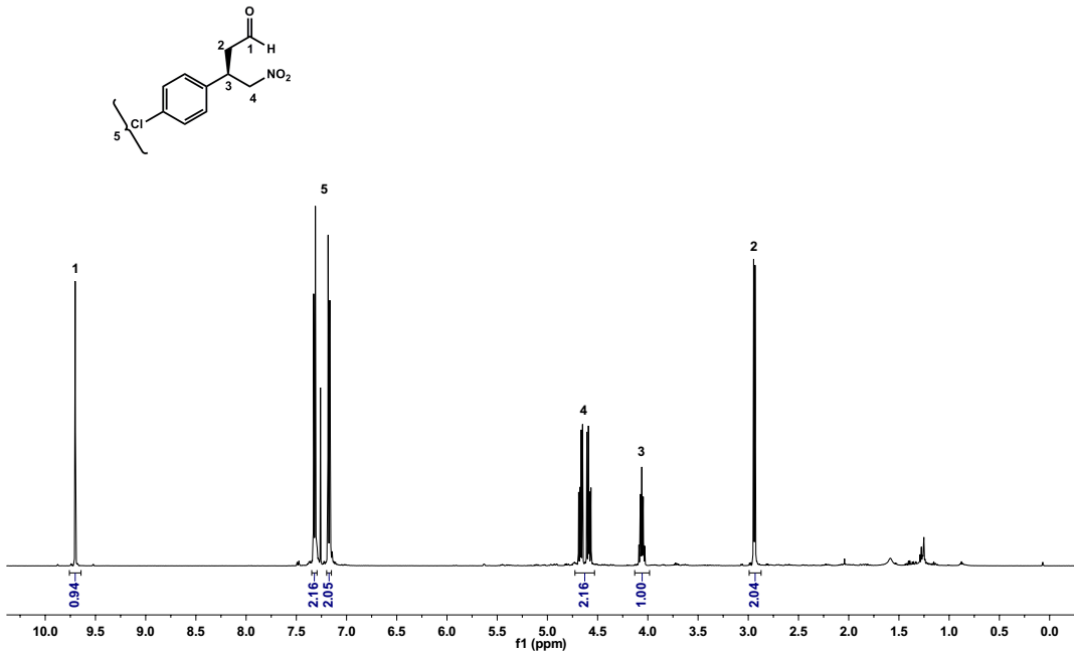

Figure S8. ^{1}H NMR spectrum of enzymatically prepared (*R*)-3-(4-chlorophenyl)-4-nitrobutanal (**3c**) (400 MHz, $CDCl_3$).

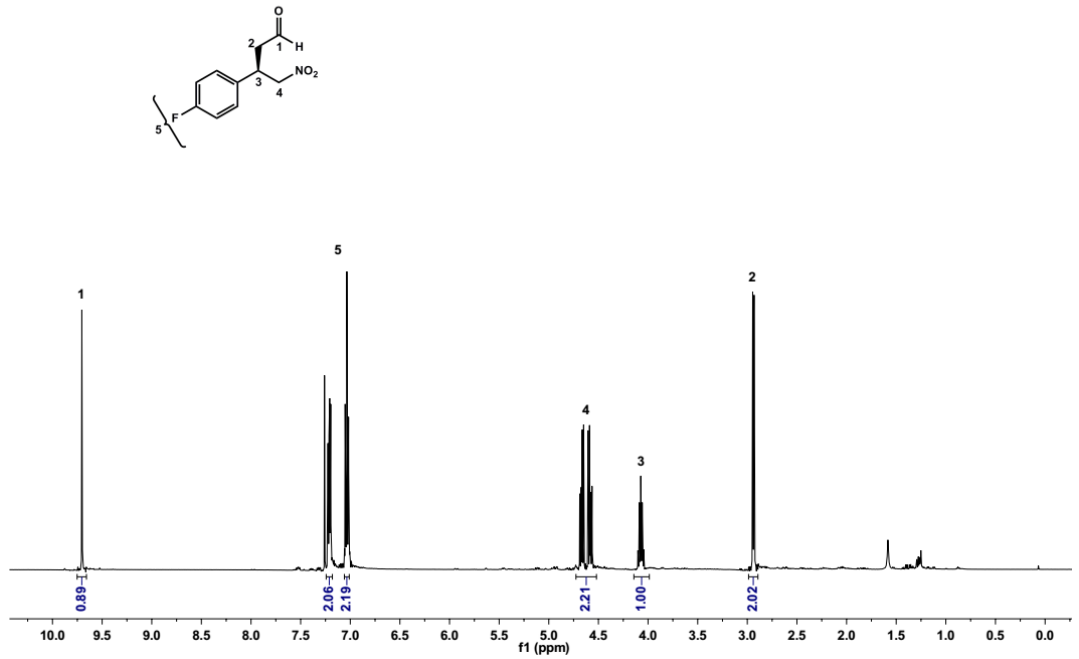

Figure S9. ^{1}H NMR spectrum of enzymatically prepared (*R*)-3-(4-fluorophenyl)-4-nitrobutanal (**3d**) (400 MHz, $CDCl_3$).

HPLC and GC chromatograms for enantiomeric excess determination of 3a-d

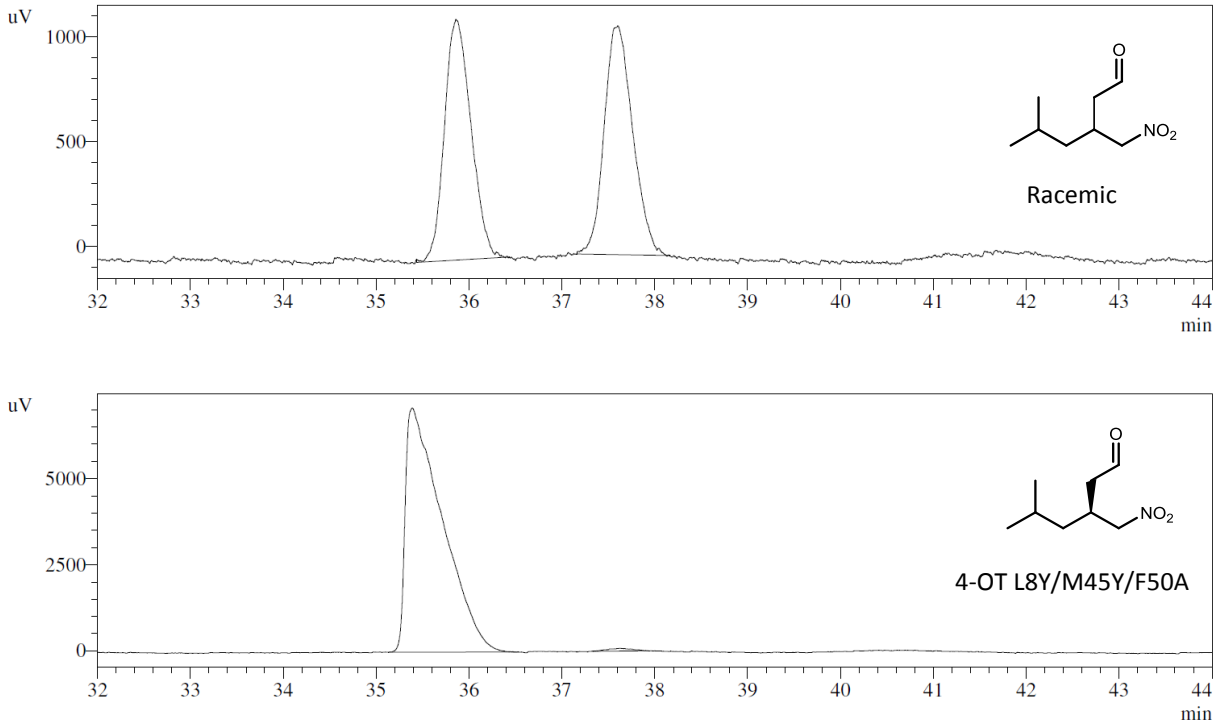

Figure S10. GC chromatograms of racemic and enzymatically obtained **3a**.

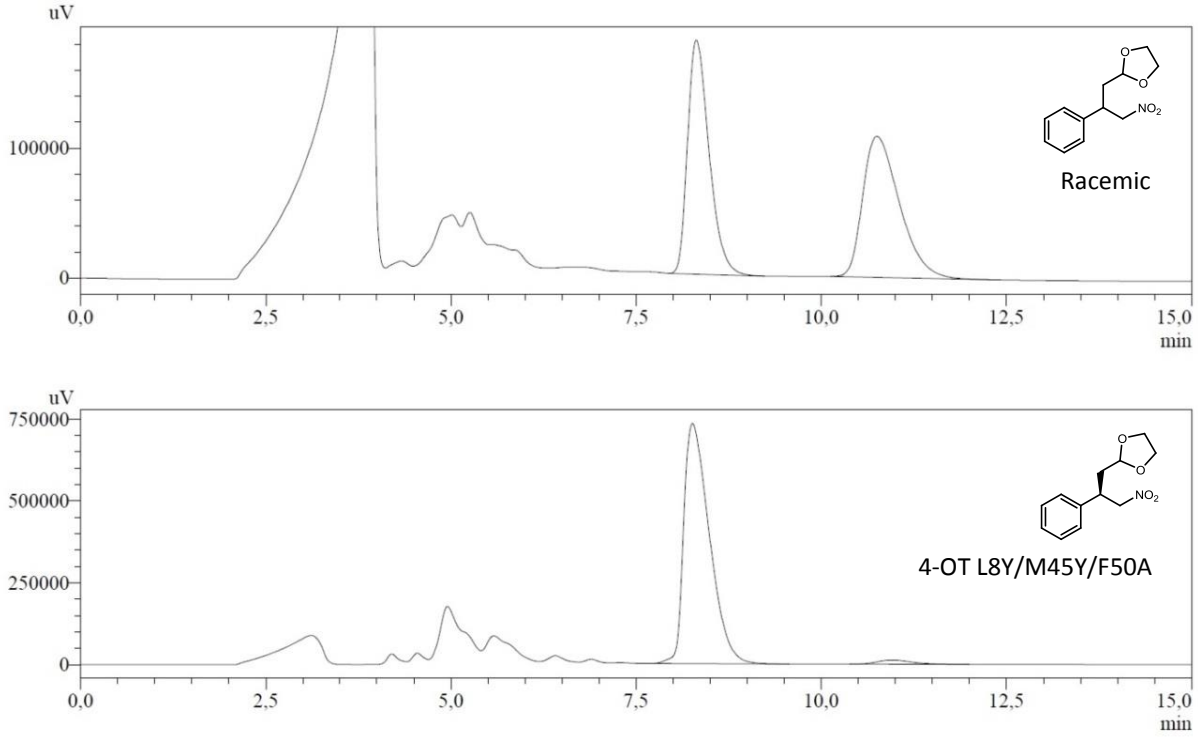

Figure S11. HPLC chromatograms of racemic and enzymatically obtained derivatized **3b**.

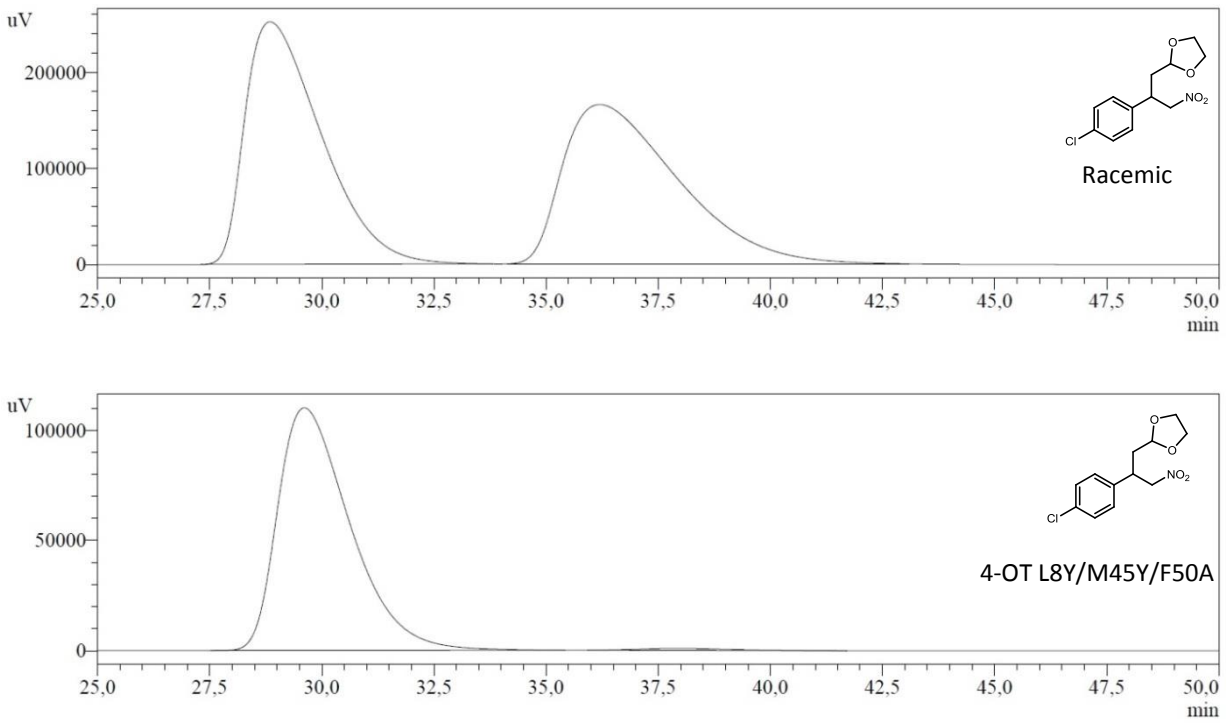

Figure S12. HPLC chromatograms of racemic and enzymatically obtained derivatized **3c**.

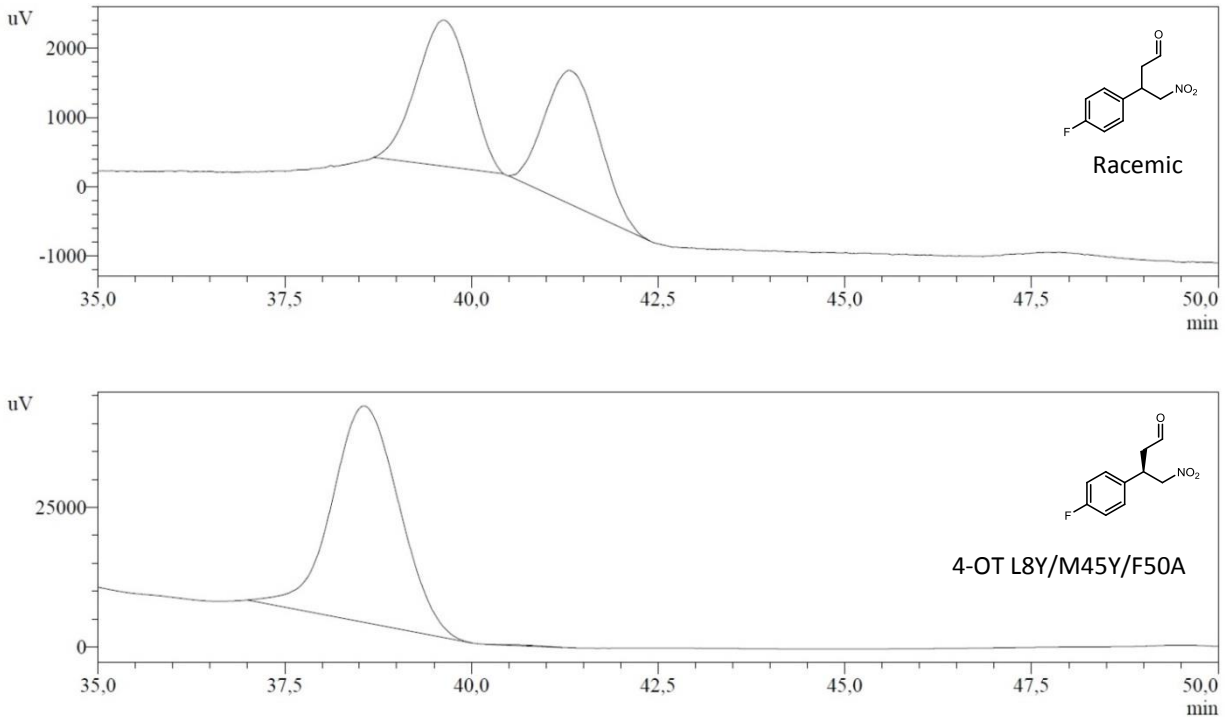

Figure S13. HPLC chromatograms of racemic and enzymatically obtained **3d**.

UV spectra and HPLC chromatograms of the one-pot synthesis of 4a-d

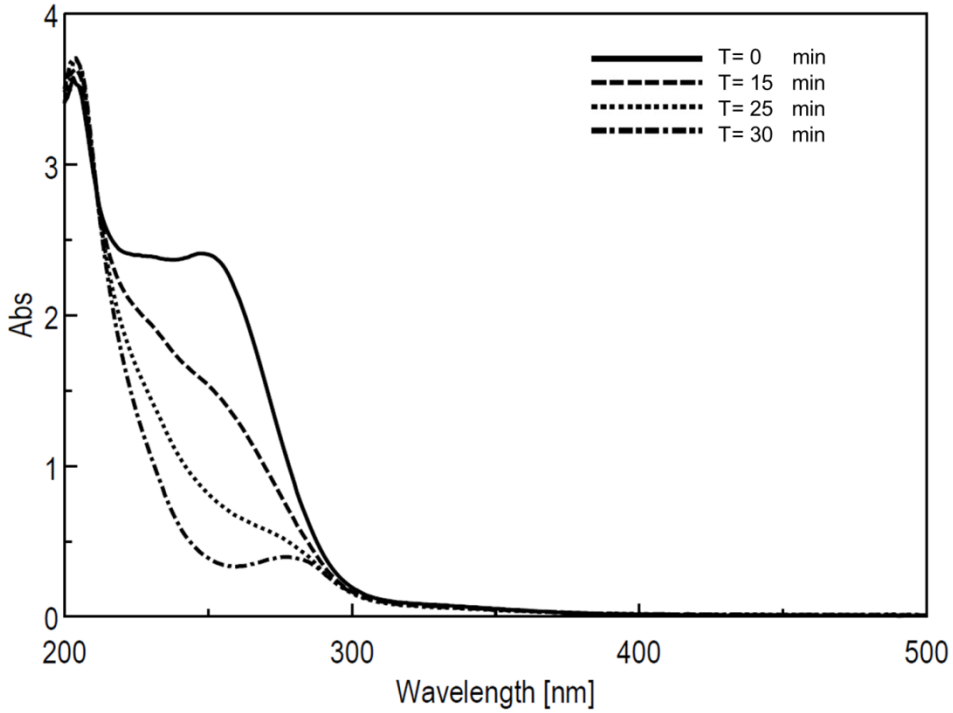

Figure S14. UV spectra showing the conversion of **2a** by 4-OT L8Y/M45Y/F50A in the first step of the enzymatic cascade.

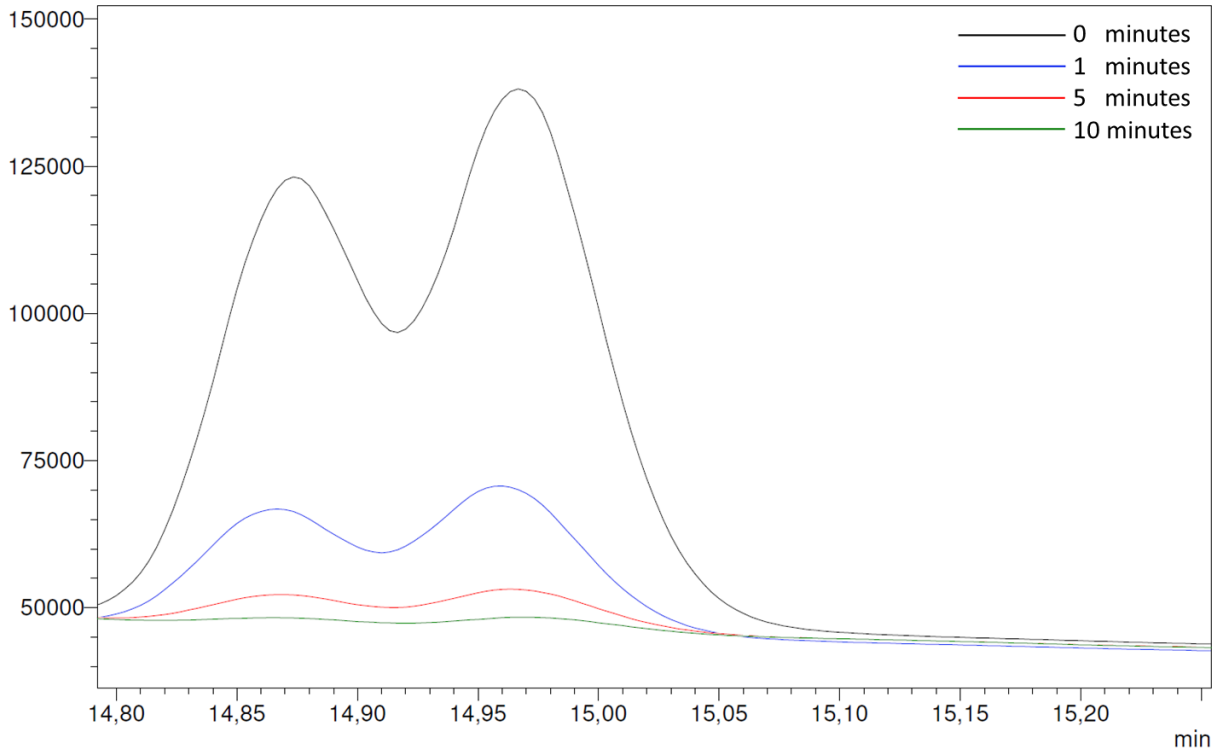

Figure S15. HPLC chromatograms showing the conversion of 4-OT L8Y/M45Y/F50A synthesized **3a** by PRO-ALDH(003) in the second step of the enzymatic cascade. The aldehyde functionality was derivatized to the corresponding (O)-benzyl oxime.

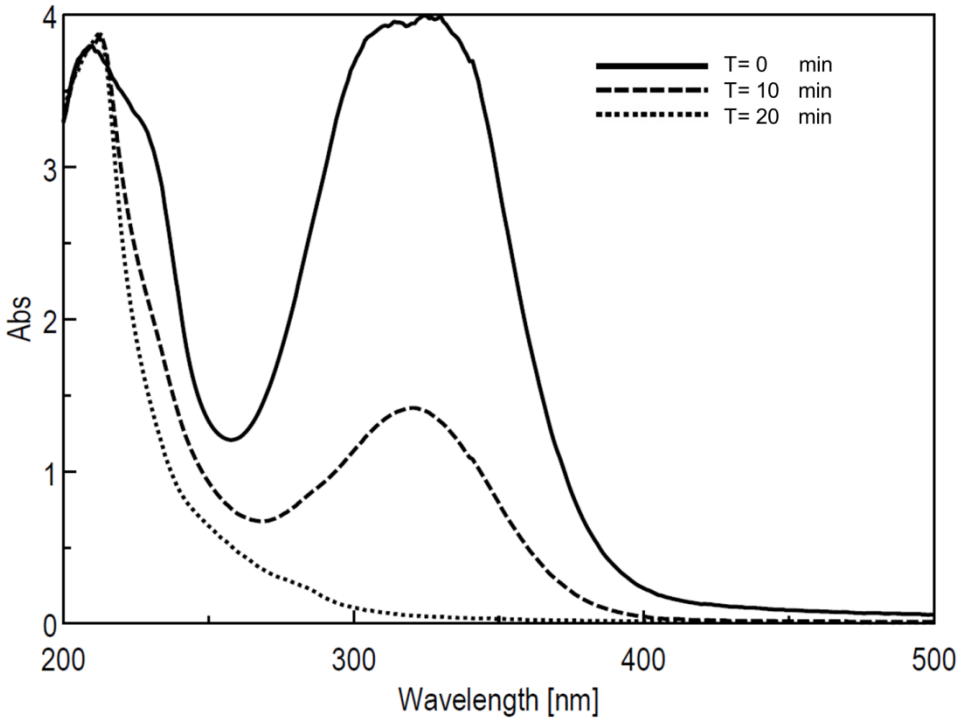

Figure S16. UV spectra showing the conversion of **2b** by 4-OT L8Y/M45Y/F50A in the first step of the enzymatic cascade.

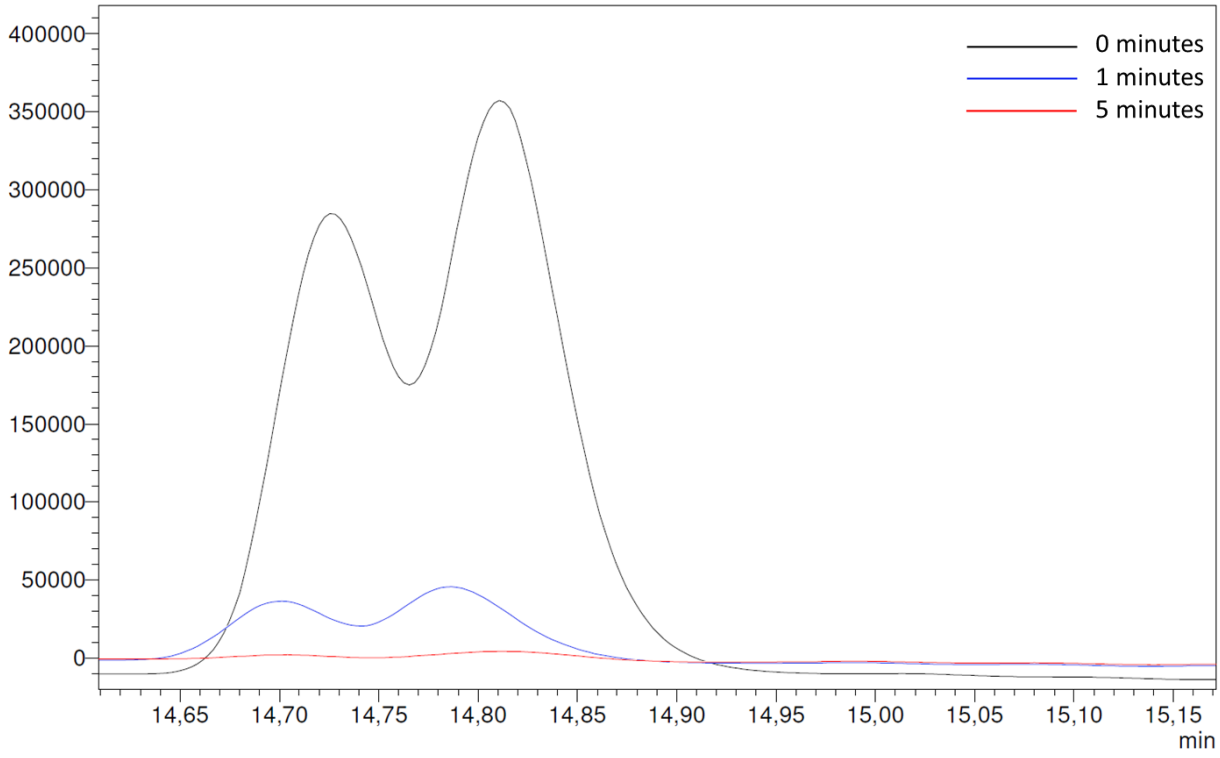

Figure S17. HPLC chromatograms showing the conversion of 4-OT L8Y/M45Y/F50A synthesized **3b** by PRO-ALDH(003) in the second step of the enzymatic cascade. The aldehyde functionality was derivatized to the corresponding (O)-benzyl oxime.

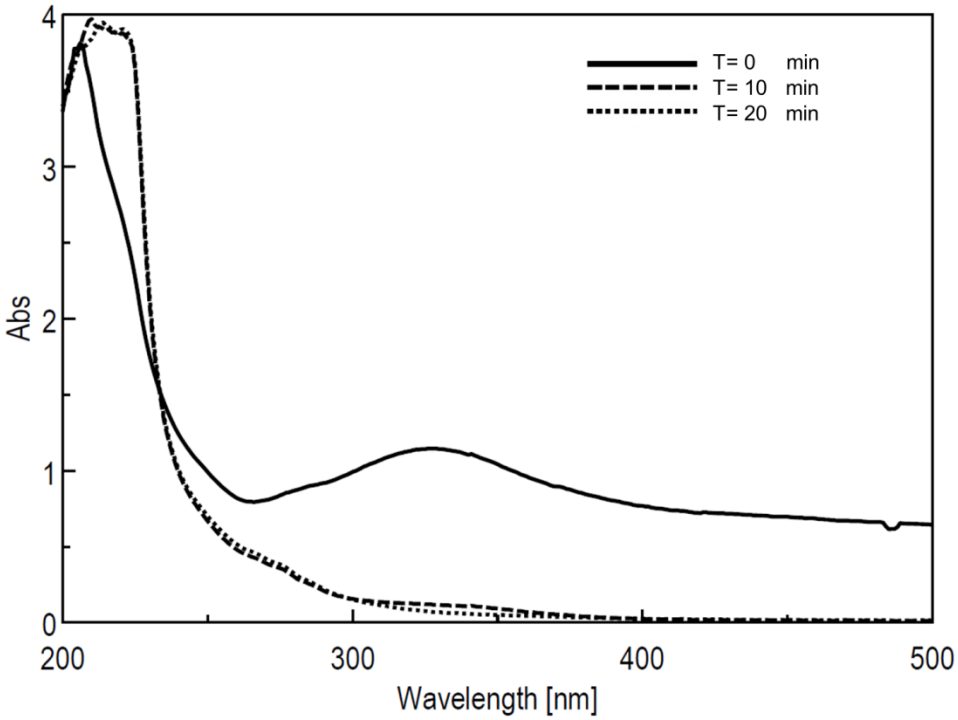

Figure S18. UV spectra showing the conversion of **2c** by 4-OT L8Y/M45Y/F50A in the first step of the enzymatic cascade.

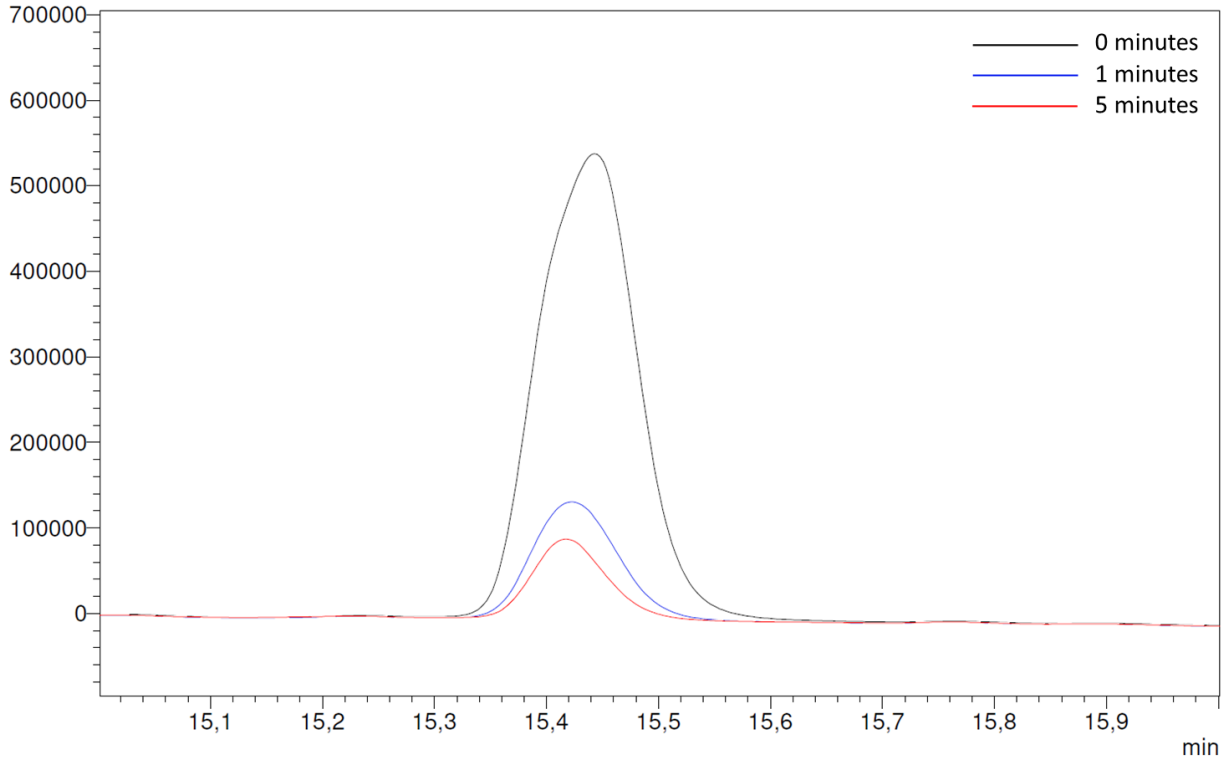

Figure S19. HPLC chromatograms showing the conversion of 4-OT L8Y/M45Y/F50A synthesized **3c** by PRO-ALDH(003) in the second step of the enzymatic cascade. The aldehyde functionality was derivatized to the corresponding (O)-benzyl oxime.

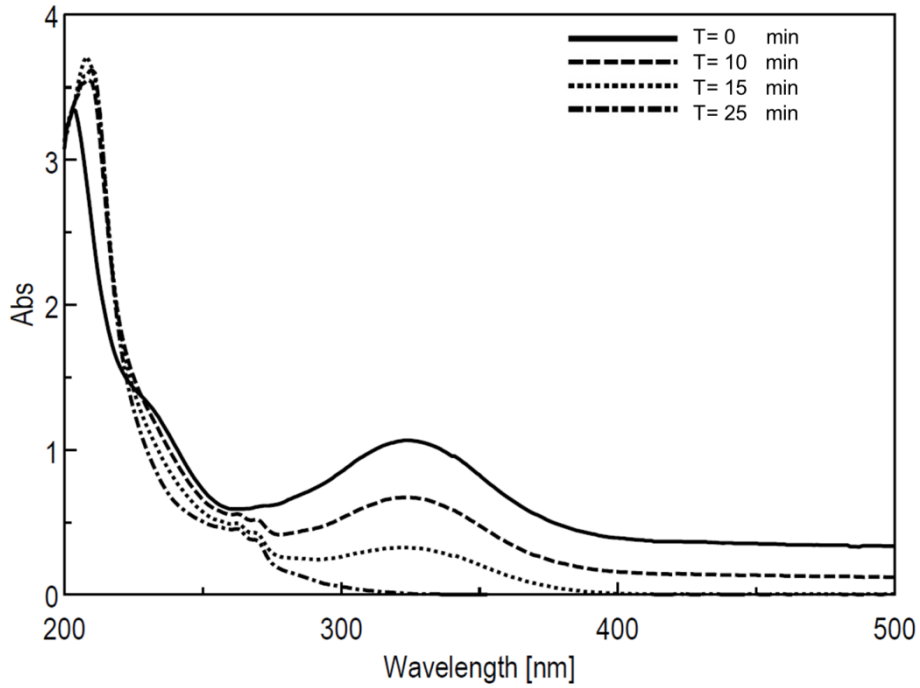

Figure S20. UV spectra showing the conversion of **2d** by 4-OT L8Y/M45Y/F50A in the first step of the enzymatic cascade.

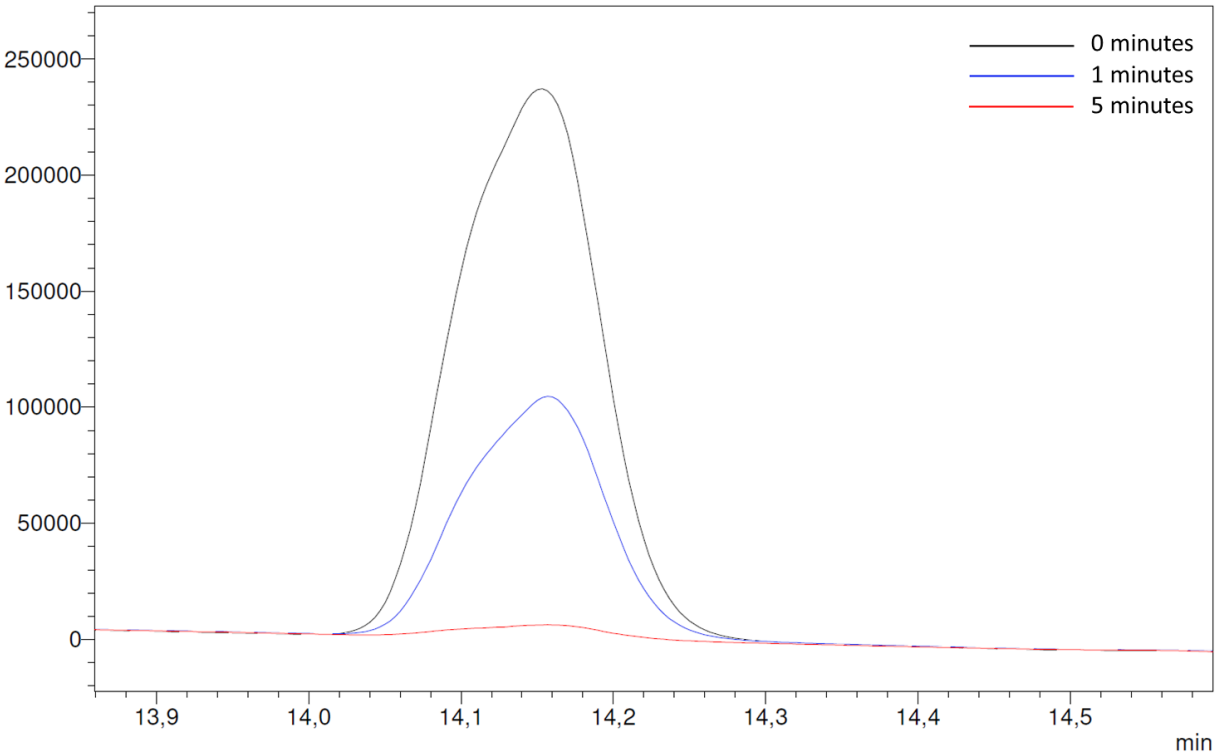

Figure S21. HPLC chromatograms showing the conversion of 4-OT L8Y/M45Y/F50A synthesized **3d** by PRO-ALDH(003) in the second step of the enzymatic cascade. The aldehyde functionality was derivatized to the corresponding (O)-benzyl oxime.

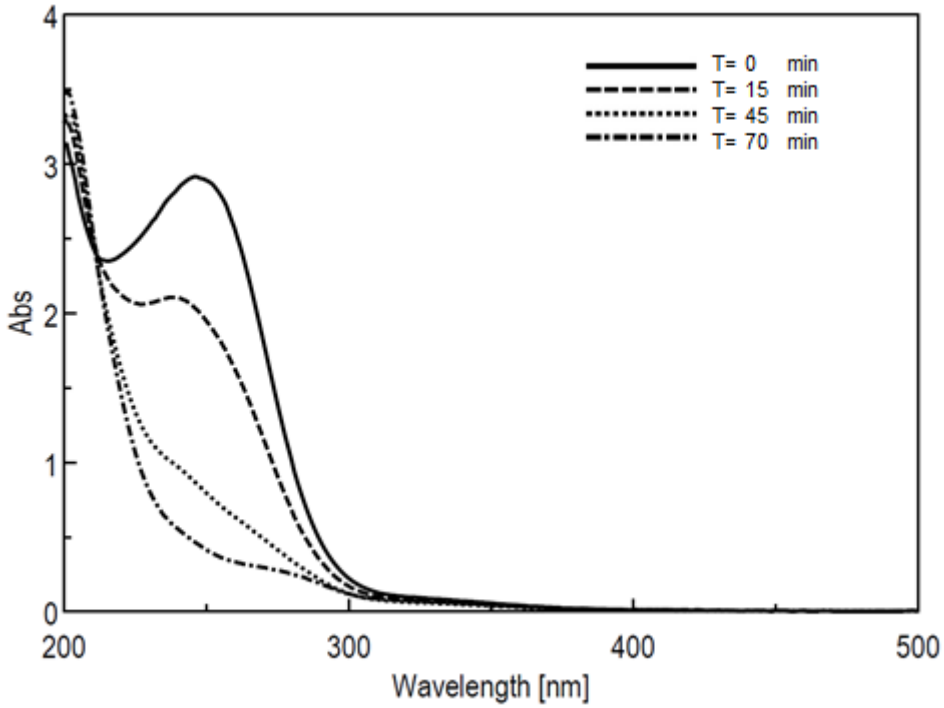

Figure S22. UV spectra showing the conversion of **2a** by 4-OT A33D in the first step of the enzymatic cascade.

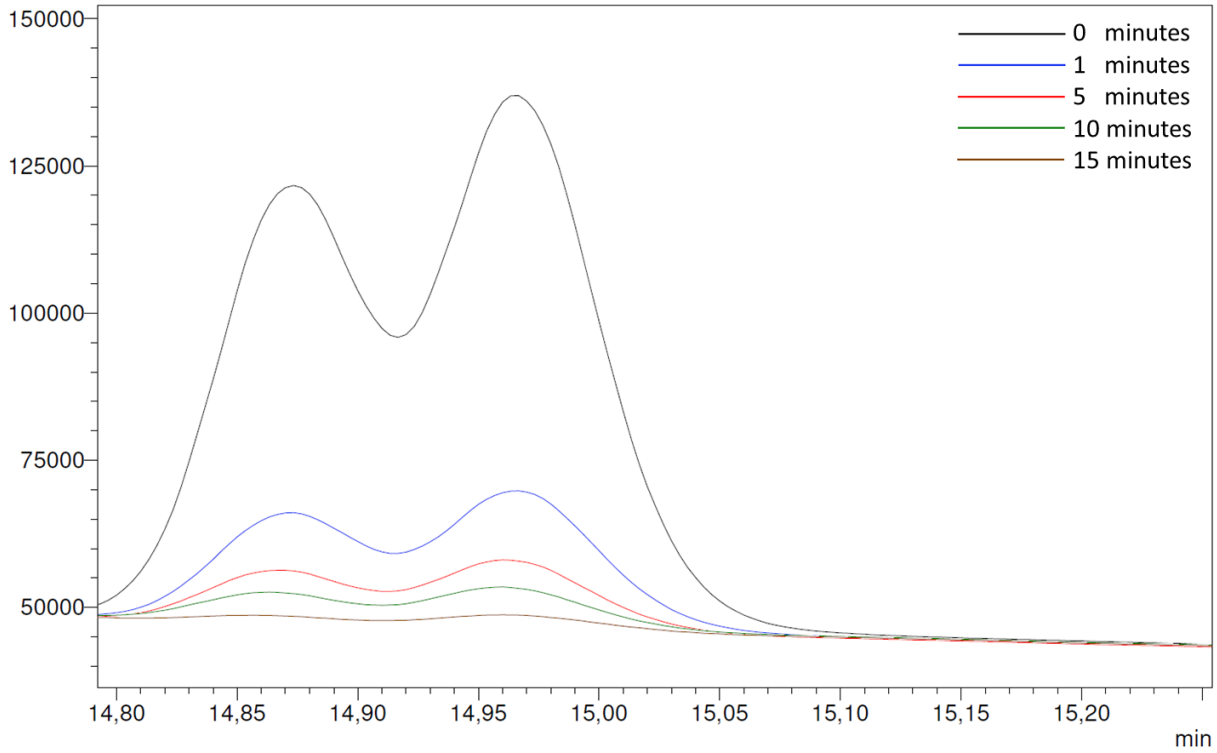

Figure S23. HPLC chromatograms showing the conversion of 4-OT A33D synthesized **3a** by PRO-ALDH(003) in the second step of the enzymatic cascade. The aldehyde functionality was derivatized to the corresponding (O)-benzyl oxime.

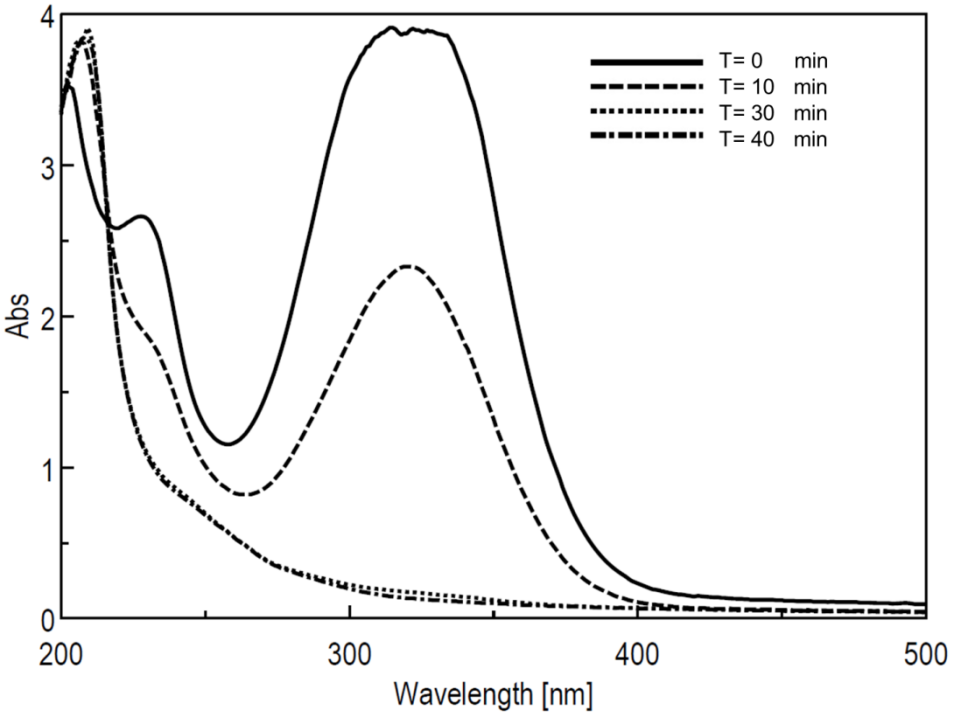

Figure S24. UV spectra showing the conversion of **2b** by 4-OT A33D in the first step of the enzymatic cascade.

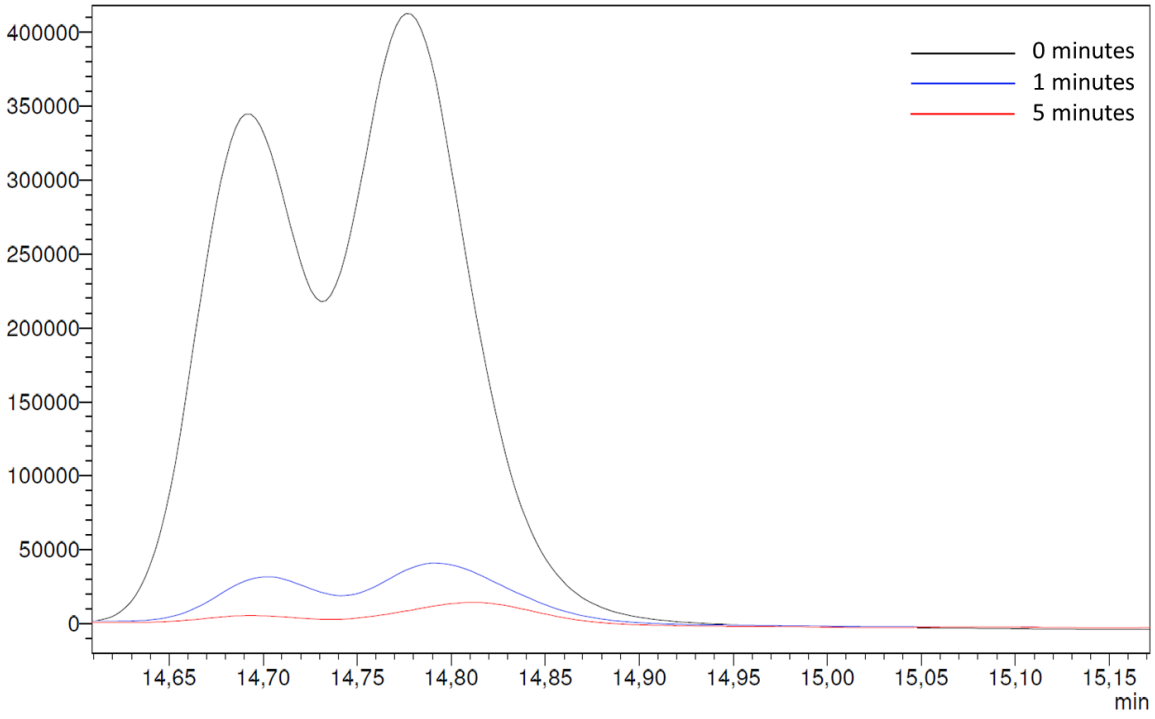

Figure S25. HPLC chromatograms showing the conversion of 4-OT A33D synthesized **3b** by PRO-ALDH(003) in the second step of the enzymatic cascade. The aldehyde functionality was derivatized to the corresponding (O)-benzyl oxime.

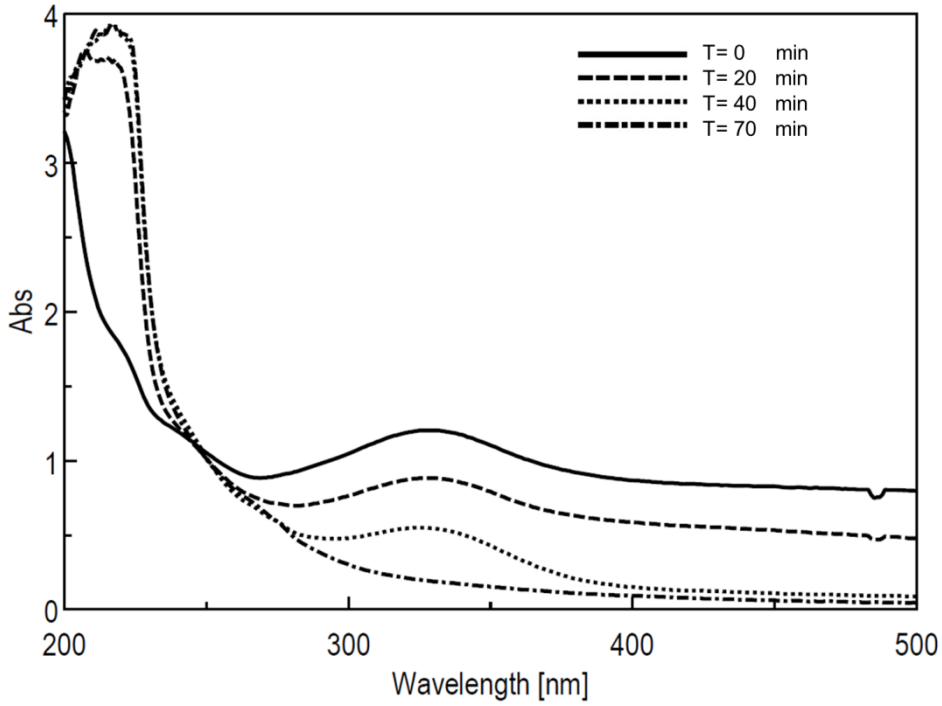

Figure S26. UV spectra showing the conversion of **2c** by 4-OT A33D in the first step of the enzymatic cascade.

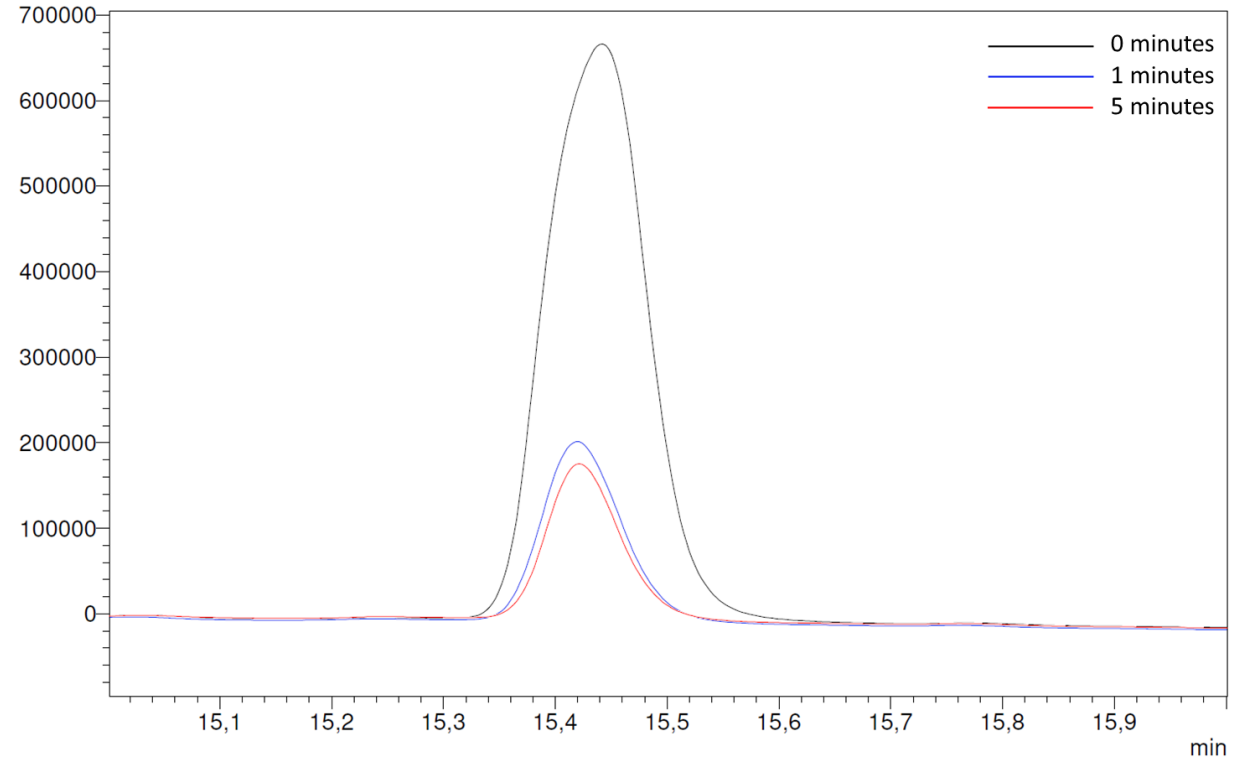

Figure S27. HPLC chromatograms showing the conversion of 4-OT A33D synthesized **3c** by PRO-ALDH(003) in the second step of the enzymatic cascade. The aldehyde functionality was derivatized to the corresponding (O)-benzyl oxime.

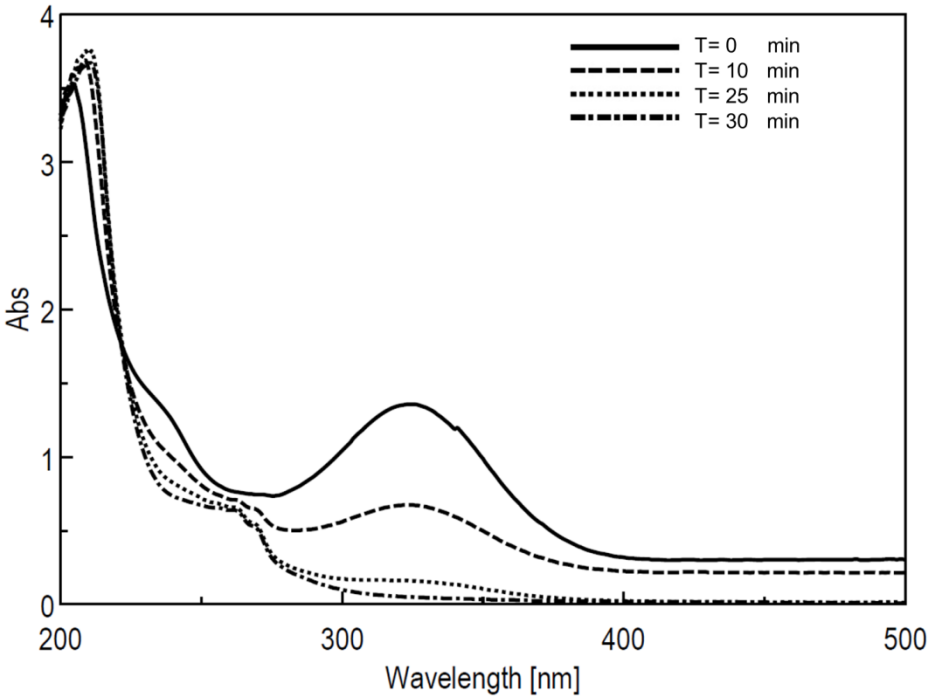

Figure S28. UV spectra showing the conversion of **2d** by 4-OT A33D in the first step of the enzymatic cascade.

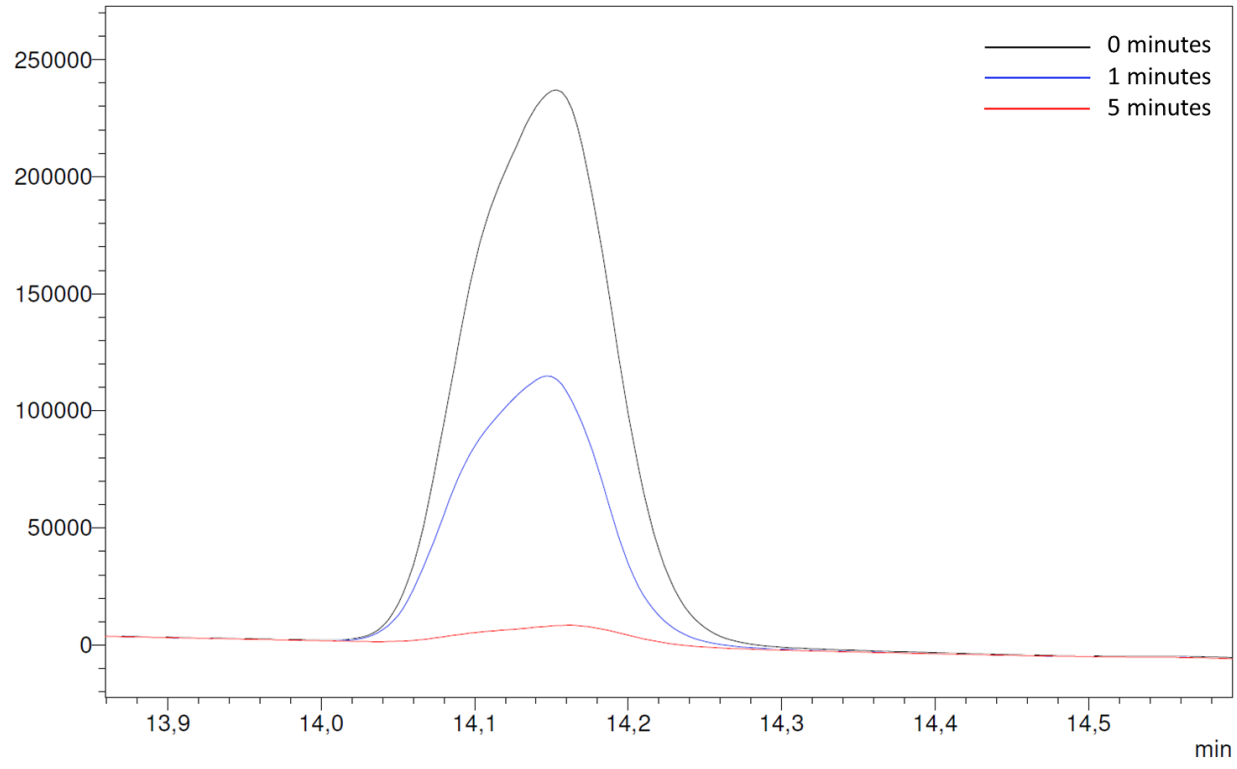

Figure S29. HPLC chromatograms showing the conversion of 4-OT A33D synthesized **3d** by PRO-ALDH(003) in the second step of the enzymatic cascade. The aldehyde functionality was derivatized to the corresponding (O)-benzyl oxime.

^{1}H NMR spectra of enzymatically obtained 4a-d

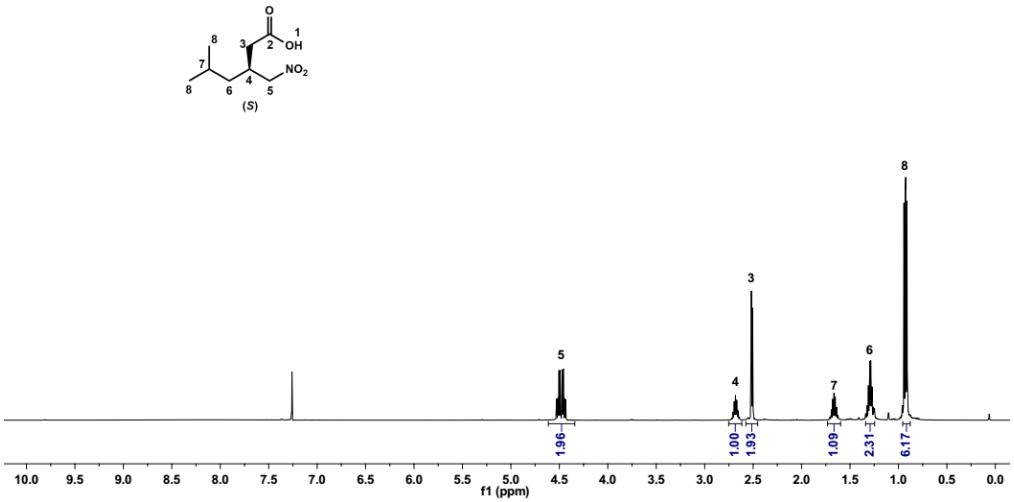

Figure S30. ^{1}H NMR spectrum of (*S*)-5-methyl-3-(nitromethyl)hexanoic acid (**4a**) obtained by 4-OT L8Y/M45Y/F50A and PRO-ALDH(003) (400 MHz, $CDCl_3$).

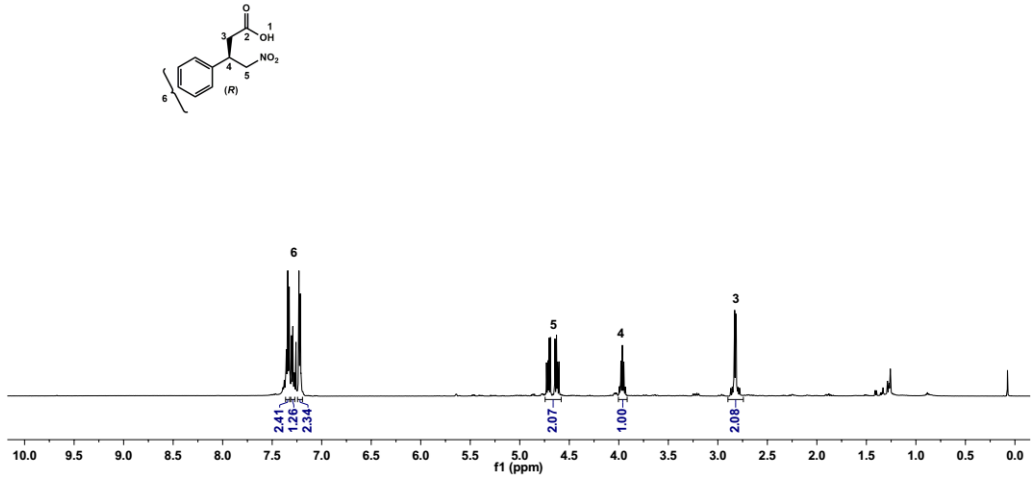

Figure S31. ^{1}H NMR spectrum of (*R*)-4-nitro-3-phenylbutanoic acid (**4b**) obtained by 4-OT L8Y/M45Y/F50A and PRO-ALDH(003) (400 MHz, $CDCl_3$).

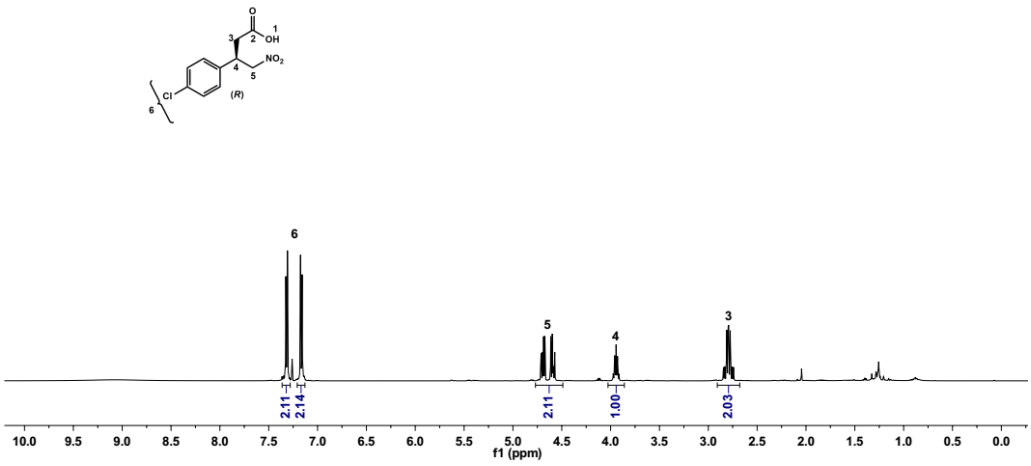

Figure S32. ^{1}H NMR spectrum of (*R*)-3-(4-chlorophenyl)-4-nitrobutanoic acid (**4c**) obtained by 4-OT L8Y/M45Y/F50A and PRO-ALDH(003) (400 MHz, $CDCl_3$).

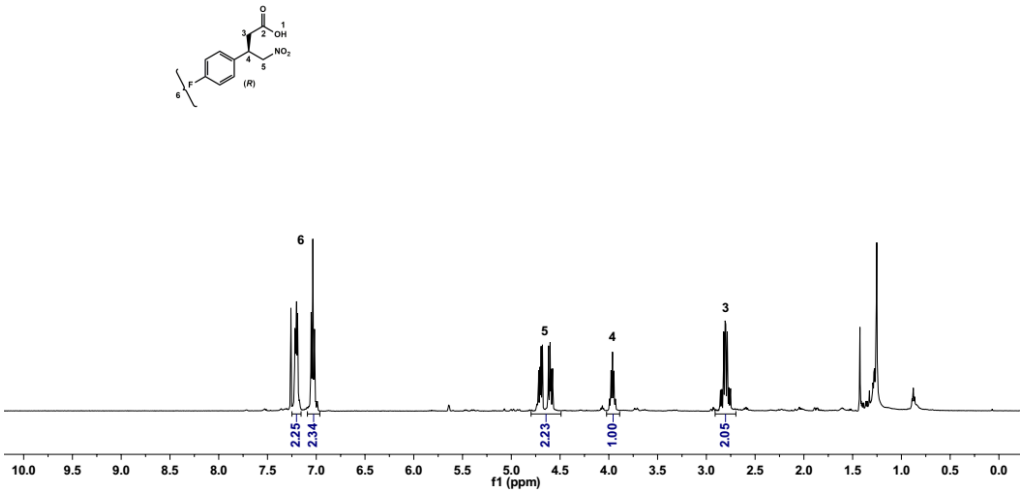

Figure S33. ^{1}H NMR spectrum of (*R*)-3-(4-fluorophenyl)-4-nitrobutanoic acid (**4d**) obtained by 4-OT L8Y/M45Y/F50A and PRO-ALDH(003) (400 MHz, $CDCl_3$).

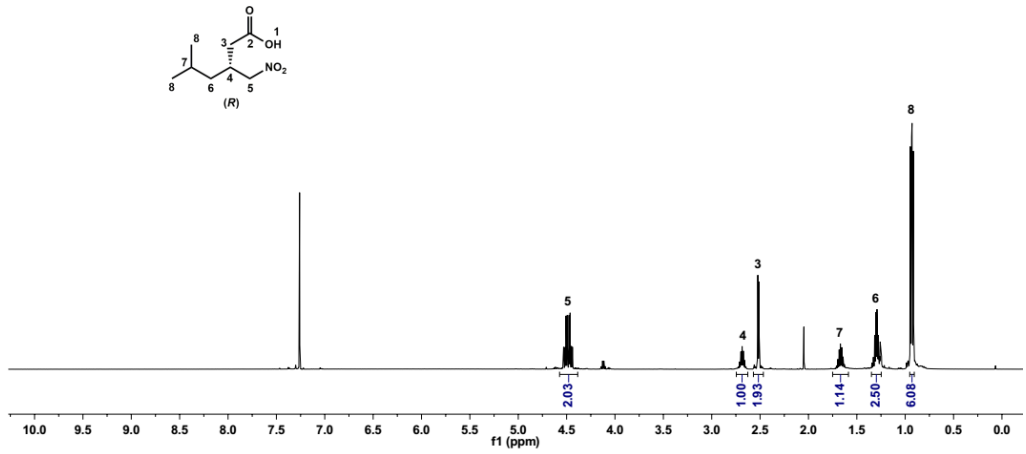

Figure S34. ^{1}H NMR spectrum of (*R*)-5-methyl-3-(nitromethyl)hexanoic acid (**4a**) obtained by 4-OT A33D and PRO-ALDH(003) (400 MHz, $CDCl_3$).

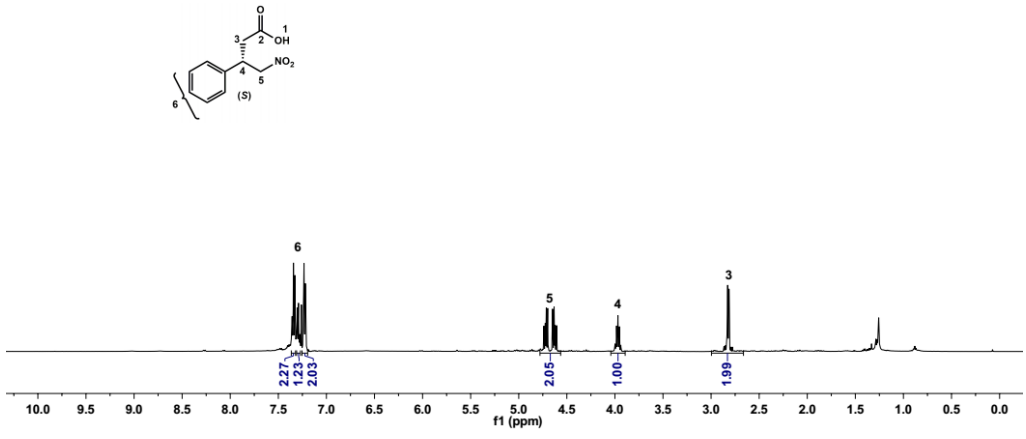

Figure S35. ^{1}H NMR spectrum of (*S*)-4-nitro-3-phenylbutanoic acid (**4b**) obtained by 4-OT A33D and PRO-ALDH(003) (400 MHz, $CDCl_3$).

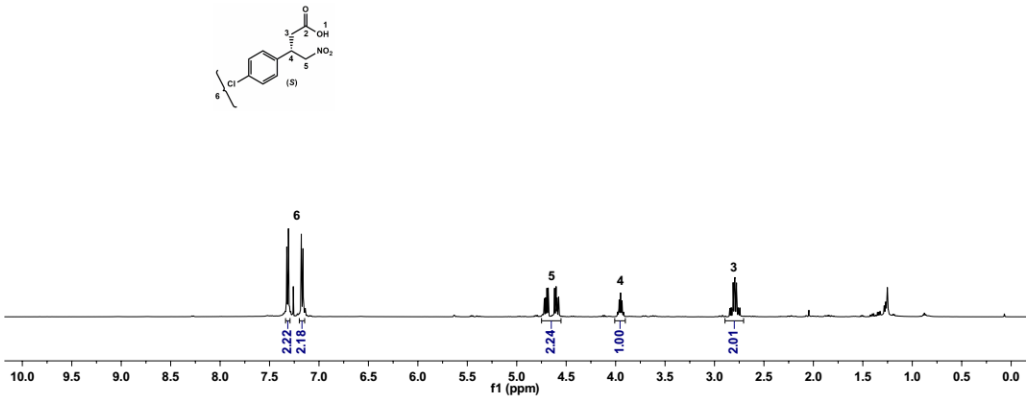

Figure S36. ^{1}H NMR spectrum of (*S*)-3-(4-chlorophenyl)-4-nitrobutanoic acid (**4c**) obtained by 4-OT A33D and PRO-ALDH(003) (400 MHz, $CDCl_3$).

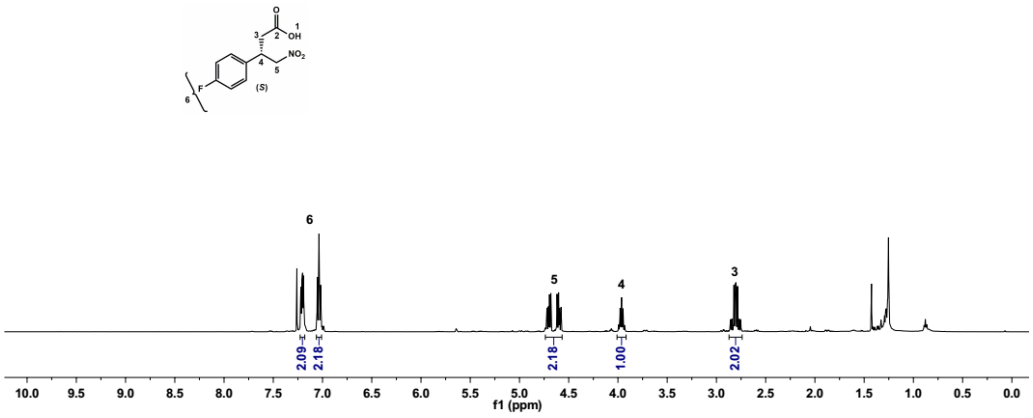

Figure S37. ^{1}H NMR spectrum of (*S*)-3-(4-fluorophenyl)-4-nitrobutanoic acid (**4d**) obtained by 4-OT A33D and PRO-ALDH(003) (400 MHz, $CDCl_3$).

^{1}H NMR spectra of racemic derivatized 4a-d

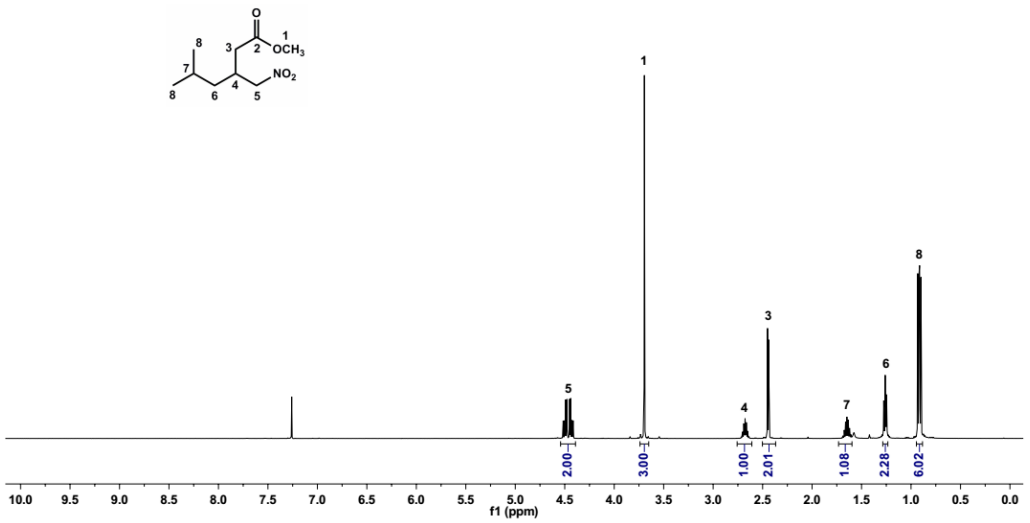

Figure S38. ^{1}H NMR spectrum of racemic methyl 5-methyl-3-(nitromethyl)hexanoate (400 MHz, $CDCl_3$).

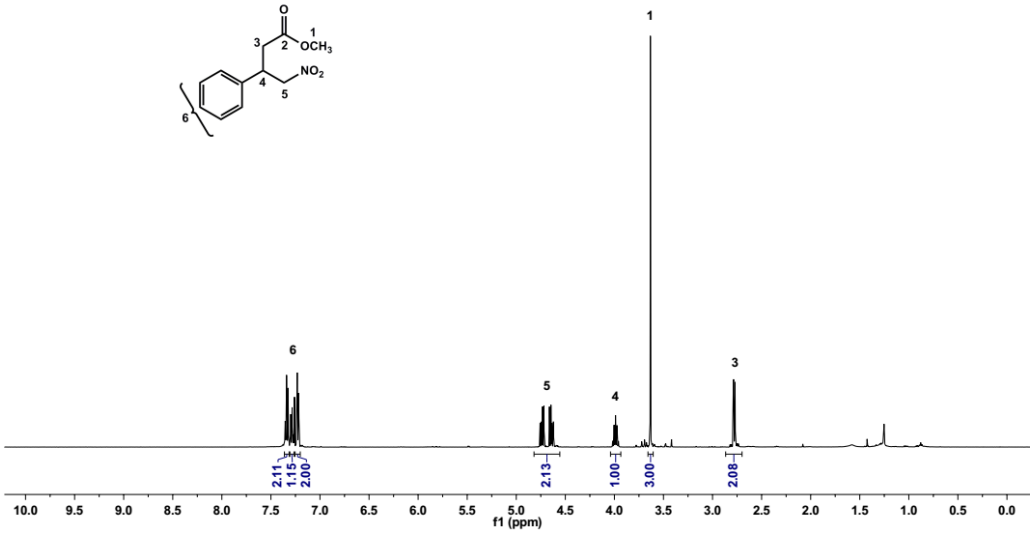

Figure S39. ^{1}H NMR spectrum of racemic methyl 4-nitro-3-phenylbutanoate (400 MHz, $CDCl_3$).

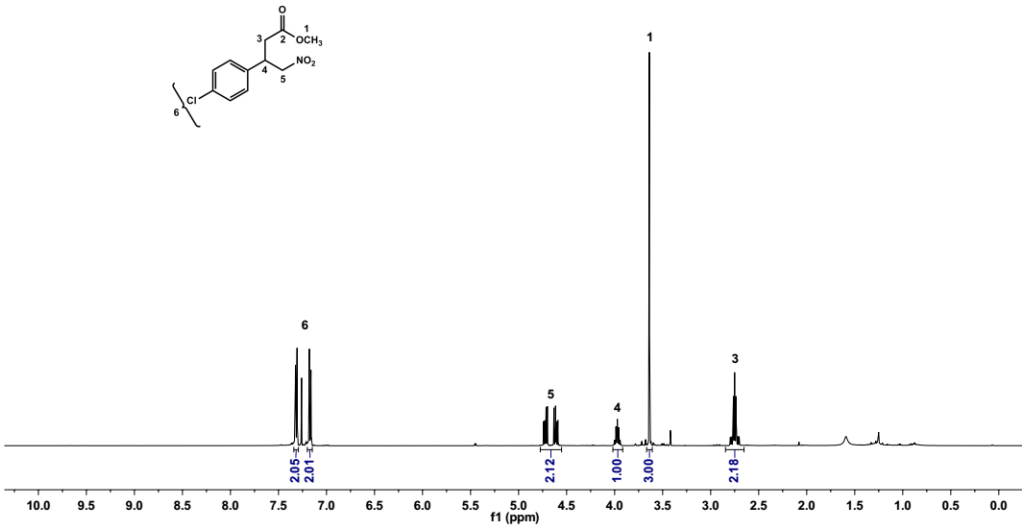

Figure S40. ^{1}H NMR spectrum of racemic methyl 3-(4-chlorophenyl)-4-nitrobutanoate (400 MHz, $CDCl_3$).

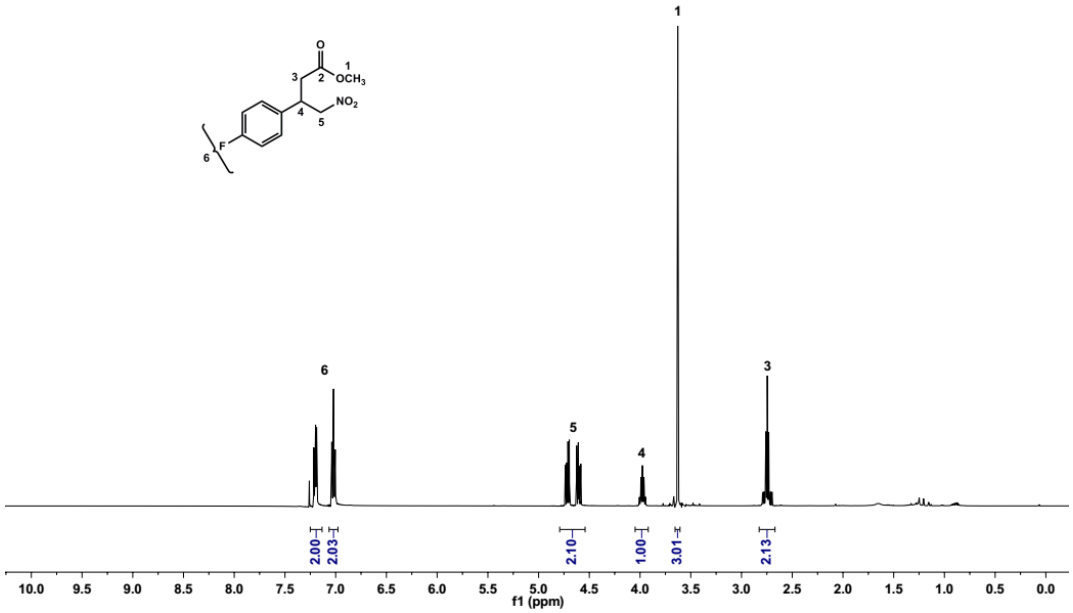

Figure S41. ^{1}H NMR spectrum of racemic methyl 3-(4-fluorophenyl)-4-nitrobutanoate (400 MHz, $CDCl_3$).

HPLC and GC chromatograms for enantiomeric excess determination of derivatized 4a-d

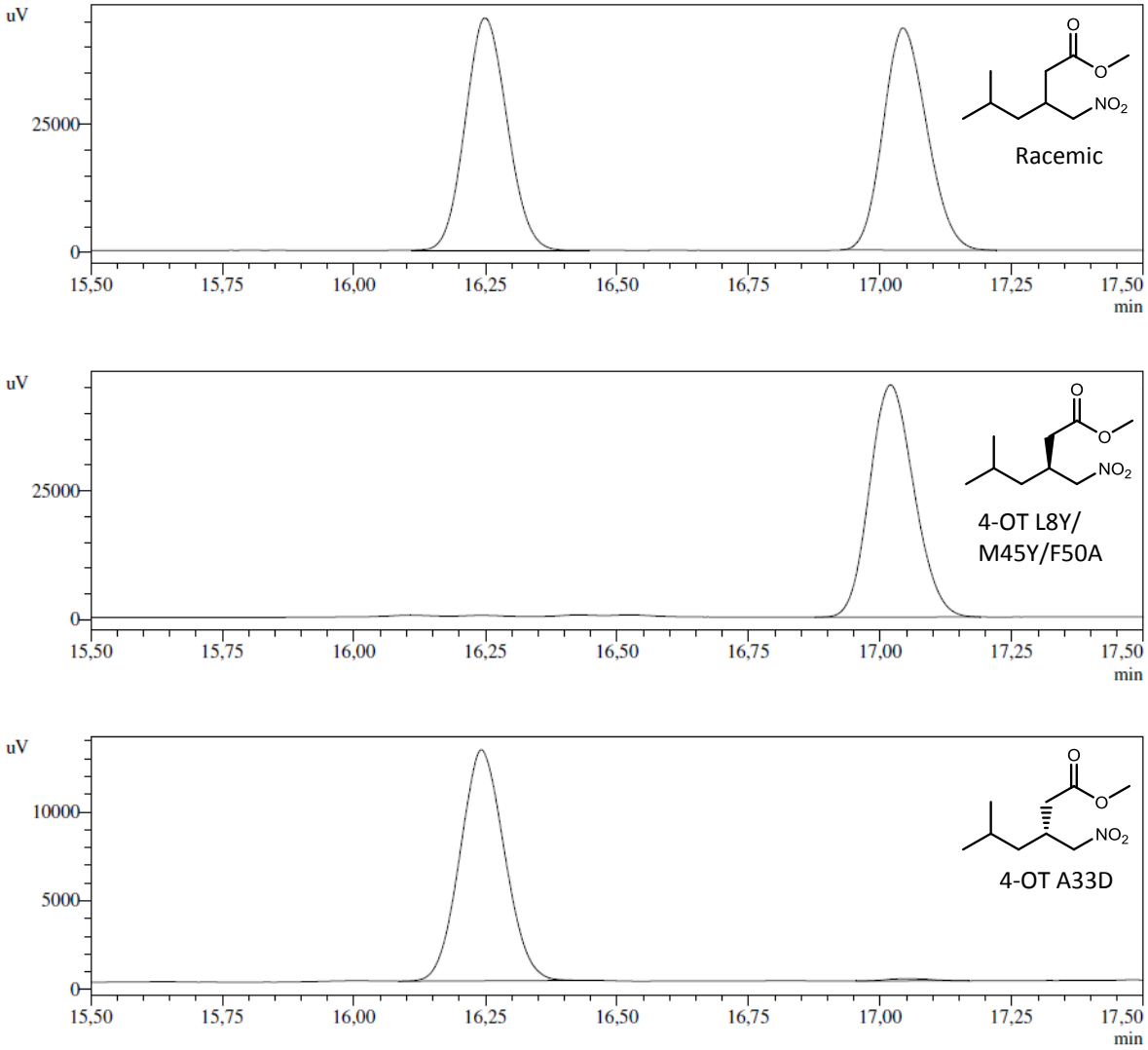

Figure S42. GC chromatograms of racemic and enzymatically obtained derivatized **4a**.

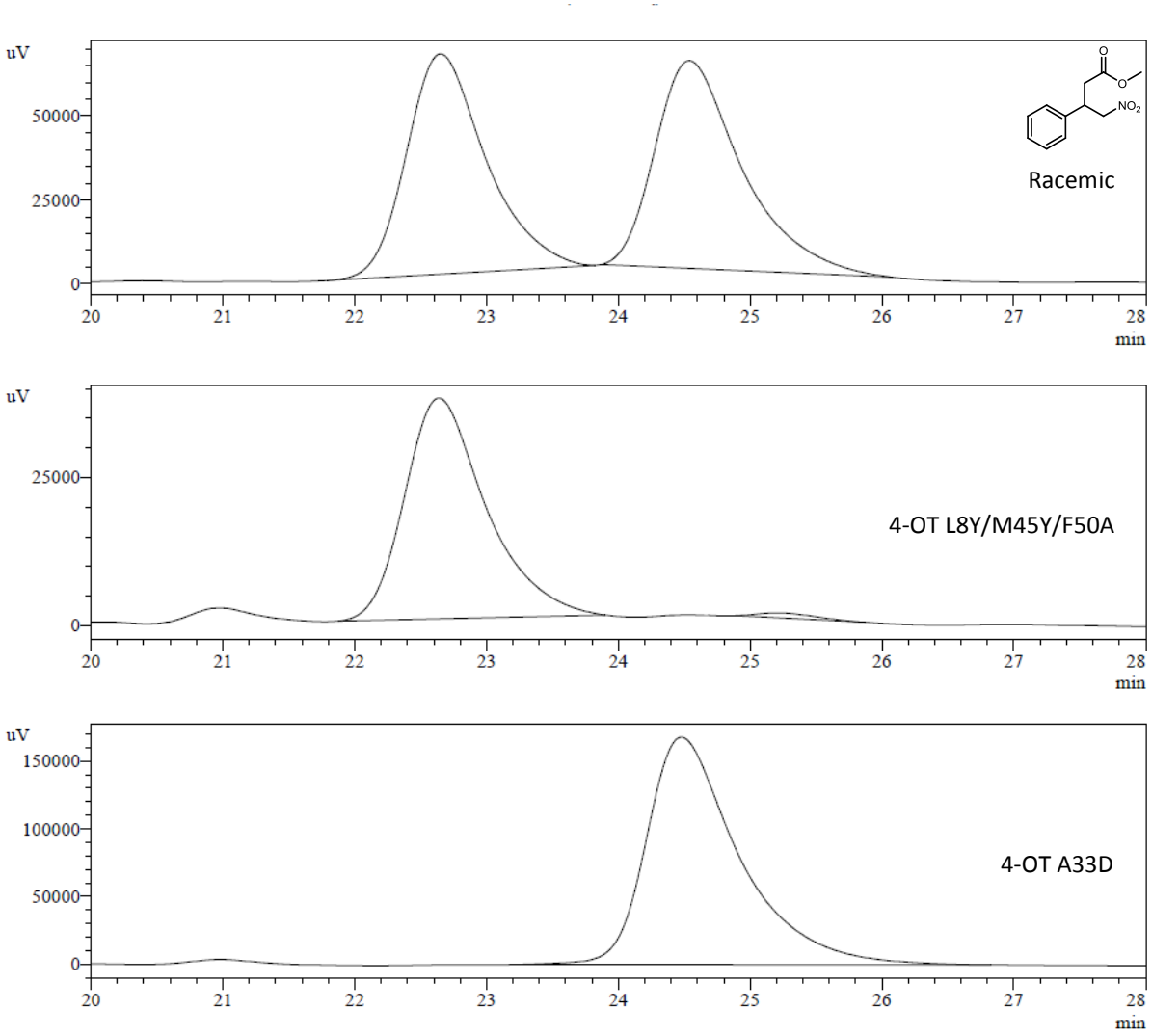

Figure S43. HPLC chromatograms of racemic or enzymatically obtained derivatized **4b**.

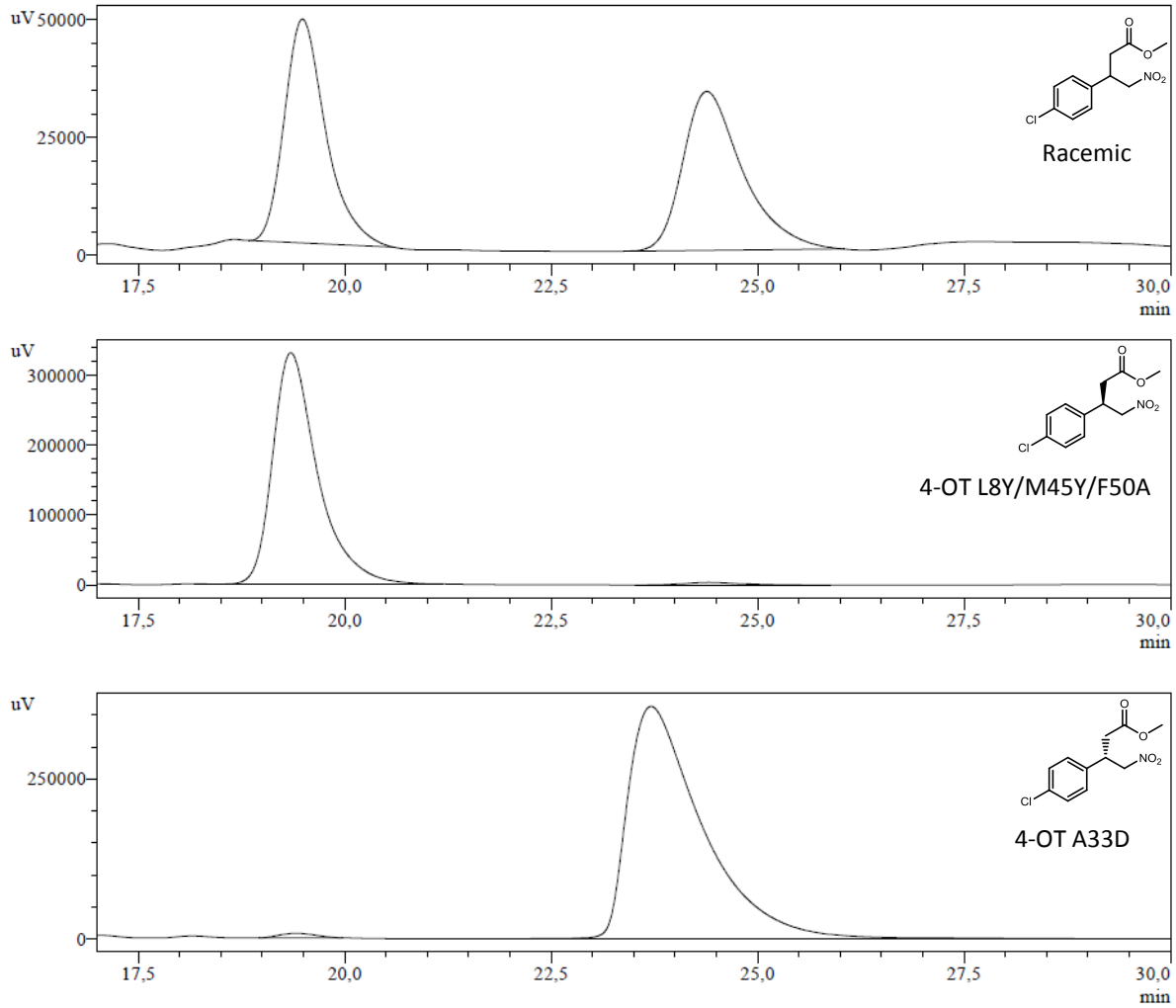

Figure S44. HPLC chromatograms of racemic and enzymatically obtained derivatized **4c**.

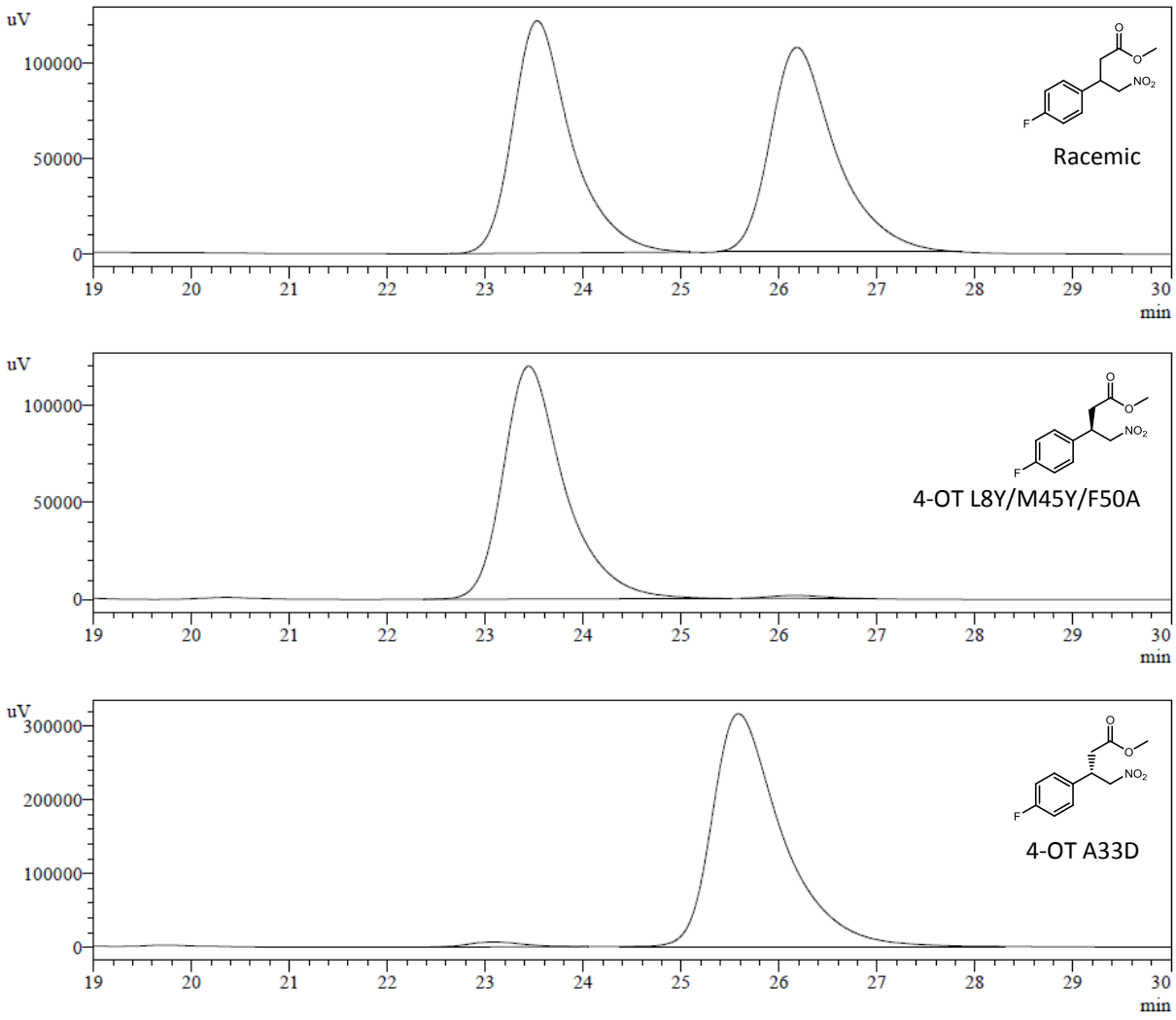

Figure S45. HPLC chromatograms of racemic and enzymatically obtained derivatized **4d**.

^{1}H NMR spectra of chemoenzymatically obtained 5a-d

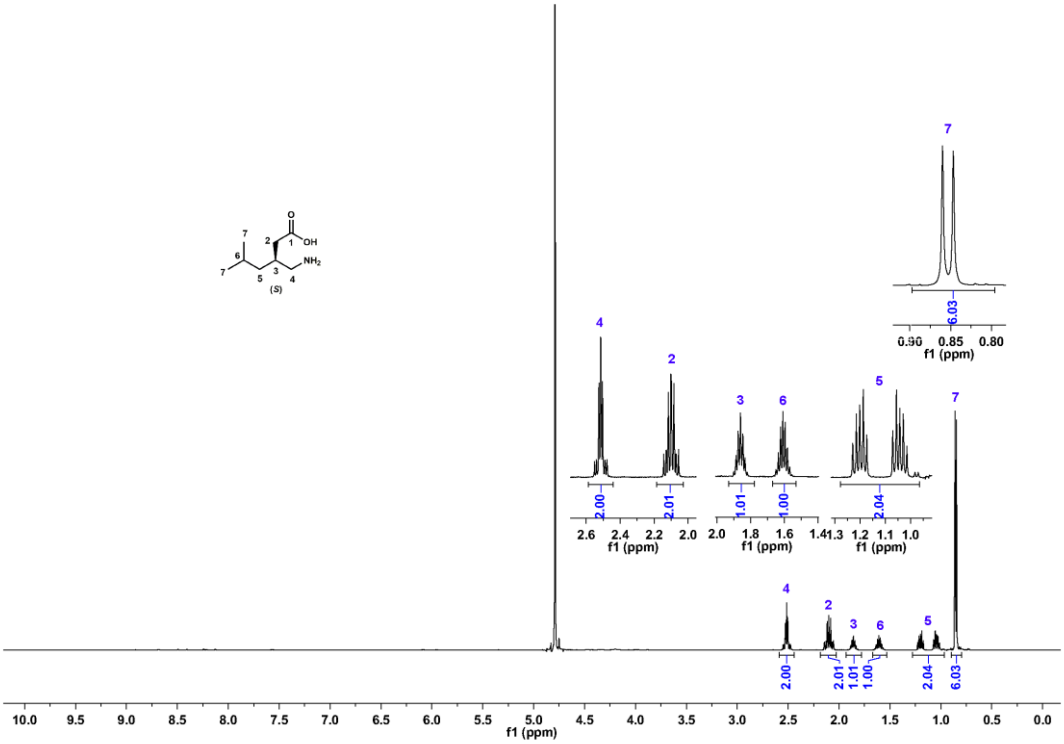

Figure S46. ^{1}H NMR spectrum of chemoenzymatically prepared (*S*)-Pregabalin (**5a**) (400 MHz, D_2O and NaOD).

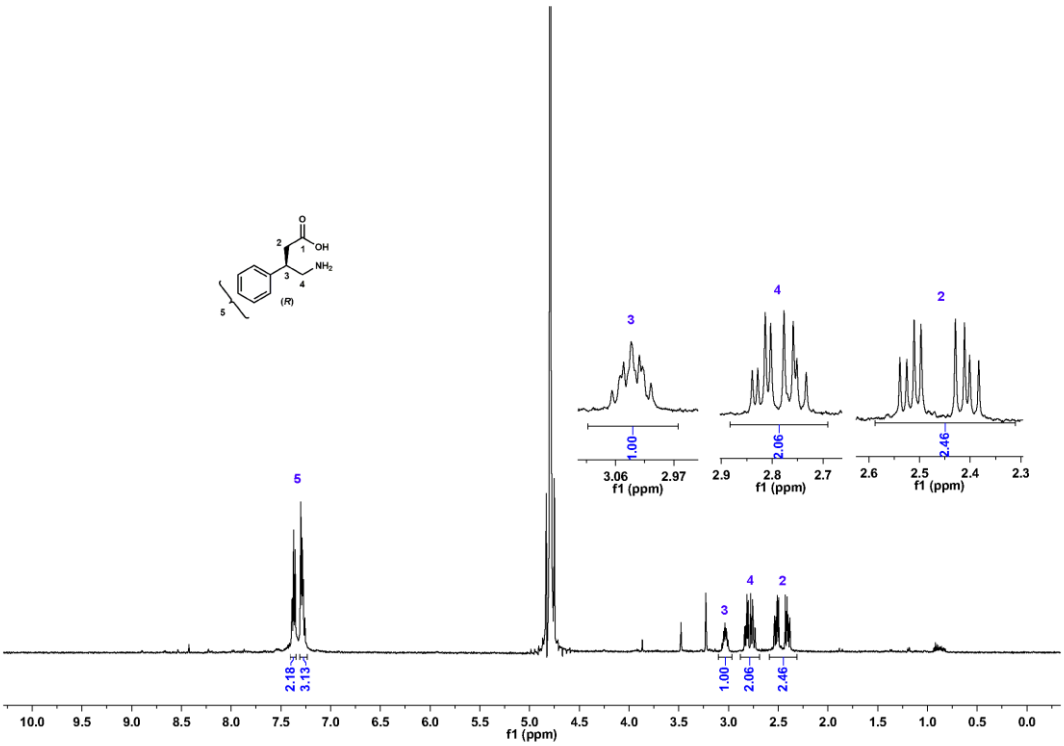

Figure S47. ^{1}H NMR spectrum of chemoenzymatically prepared (*R*)-Phenibut (**5b**) (400 MHz, D_2O and NaOD).

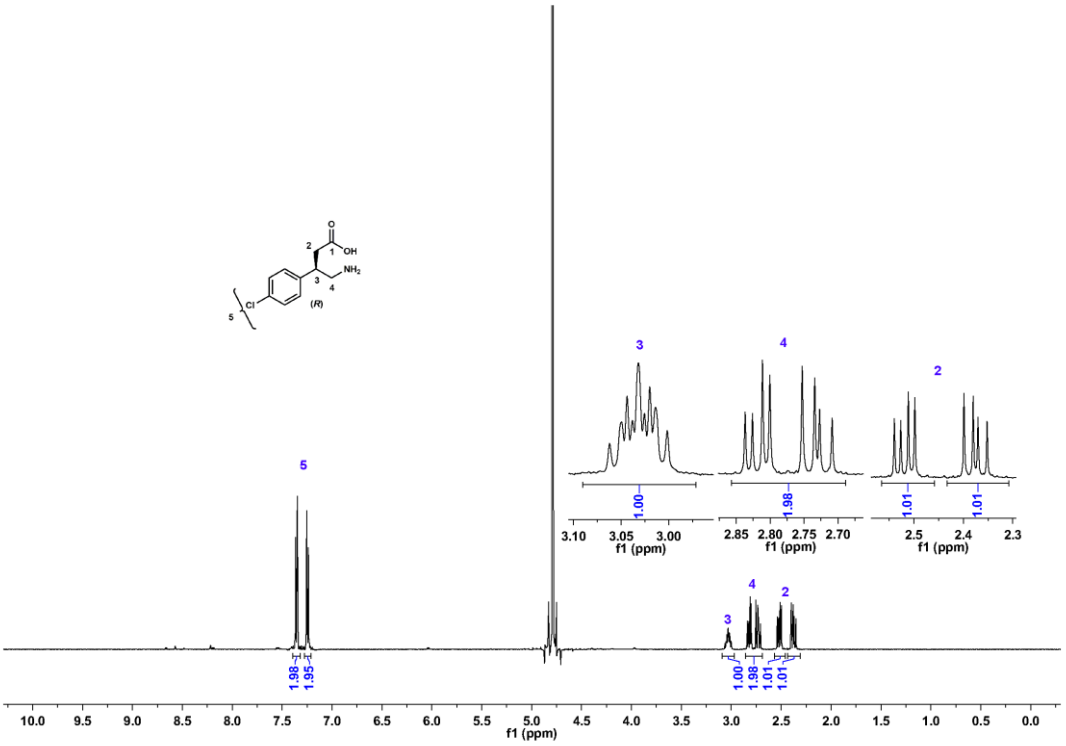

Figure S48. ^{1}H NMR spectrum of chemoenzymatically prepared (*R*)-Baclofen (**5c**) (400 MHz, D_2O and NaOD).

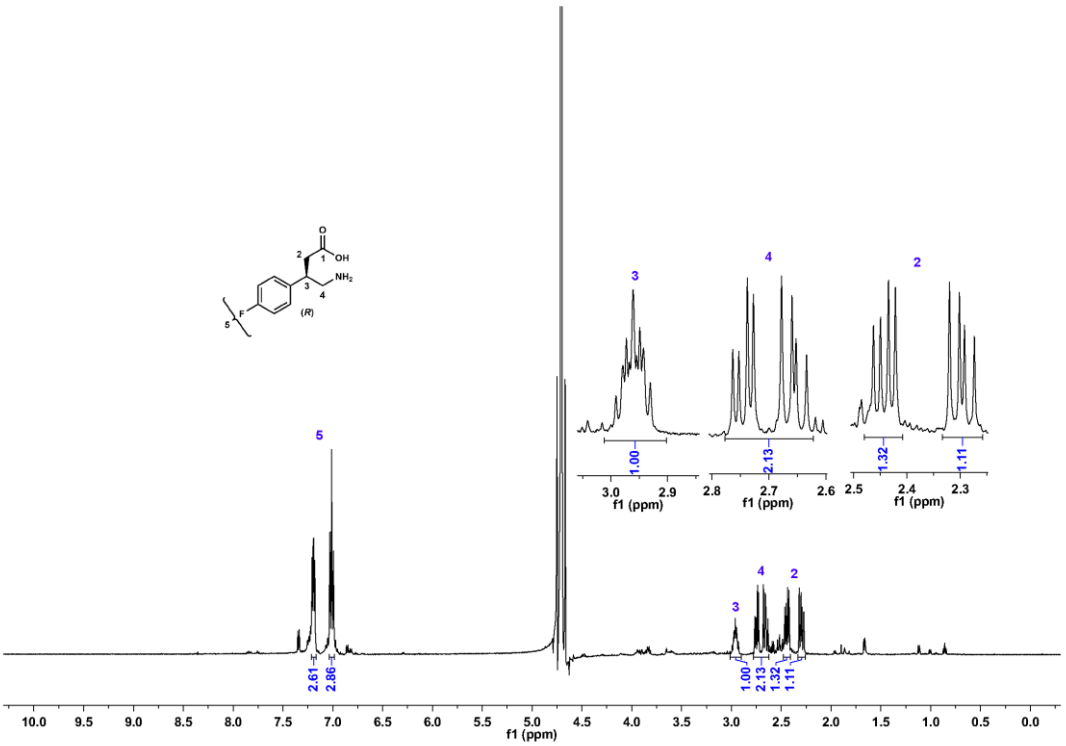

Figure S49. ^{1}H NMR spectrum of chemoenzymatically prepared fluorophenibut (**5d**) (400 MHz, D_2O and NaOD).

HPLC chromatograms for enantiomeric excess determination of derivatized 5a-d

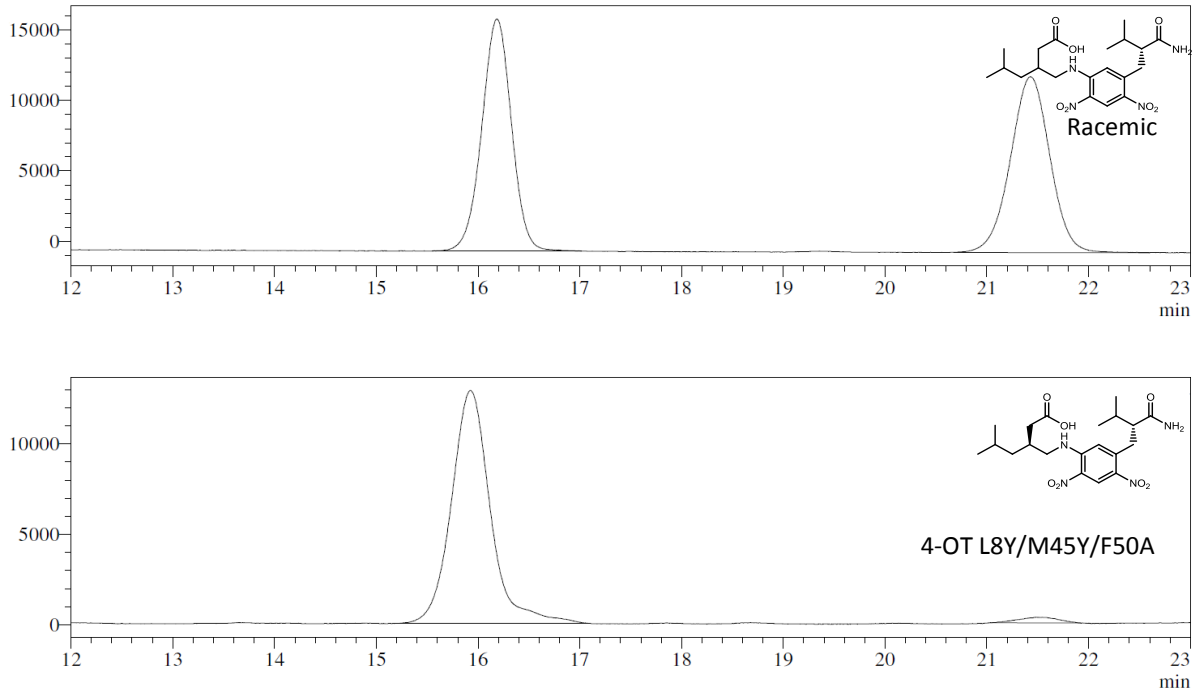

Figure S50. HPLC chromatograms of racemic and chemoenzymatically obtained derivatized **5a**.

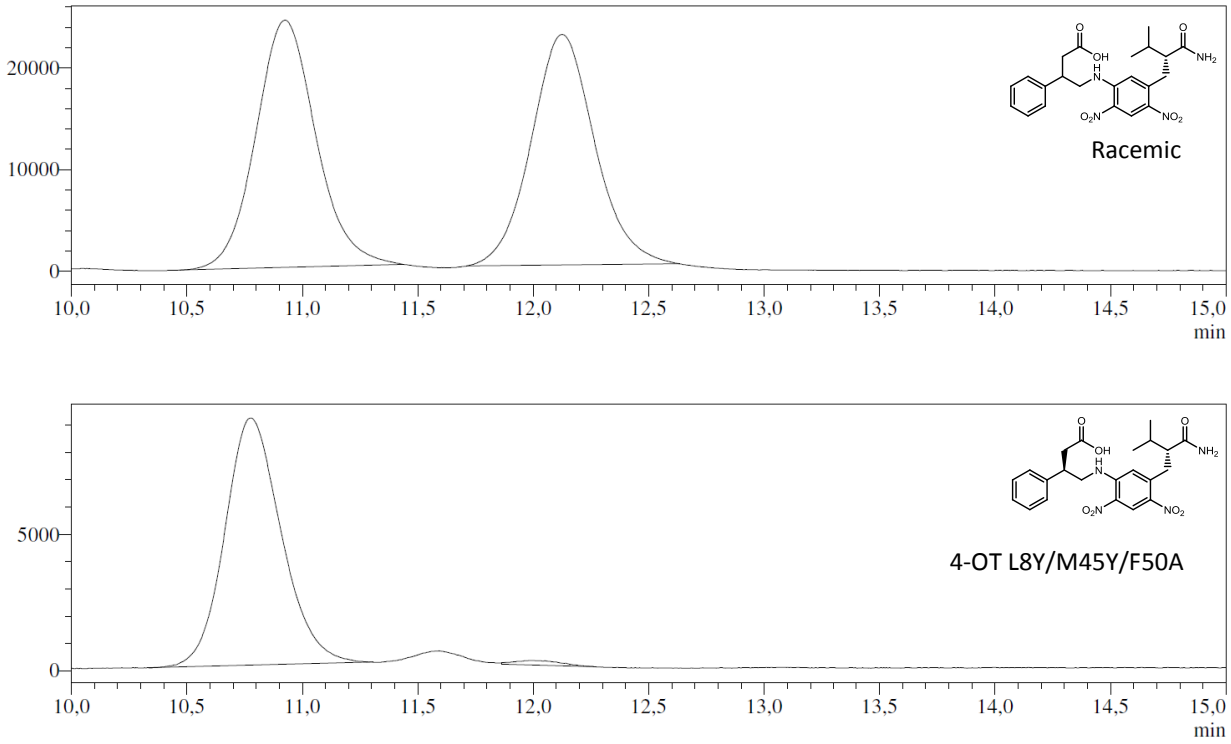

Figure S51. HPLC chromatograms of racemic and chemoenzymatically obtained derivatized **5b**.

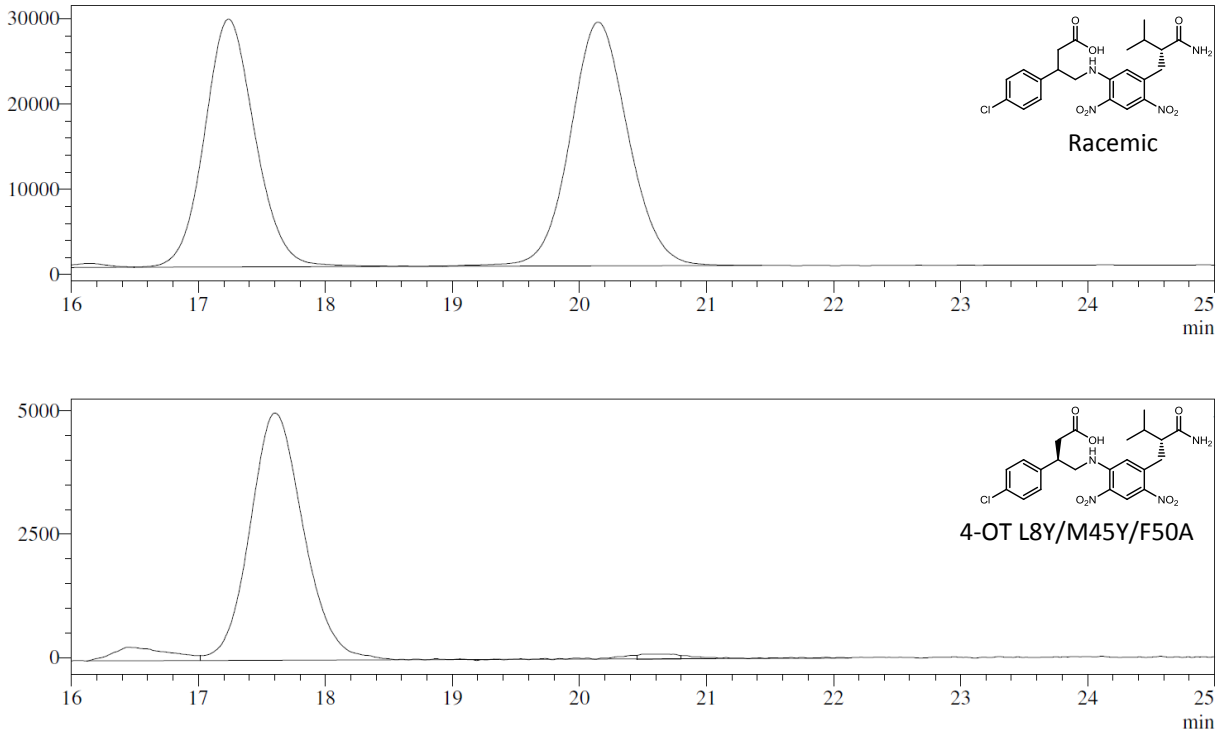

Figure S52. HPLC chromatograms of racemic and chemoenzymatically obtained derivatized **5c**.

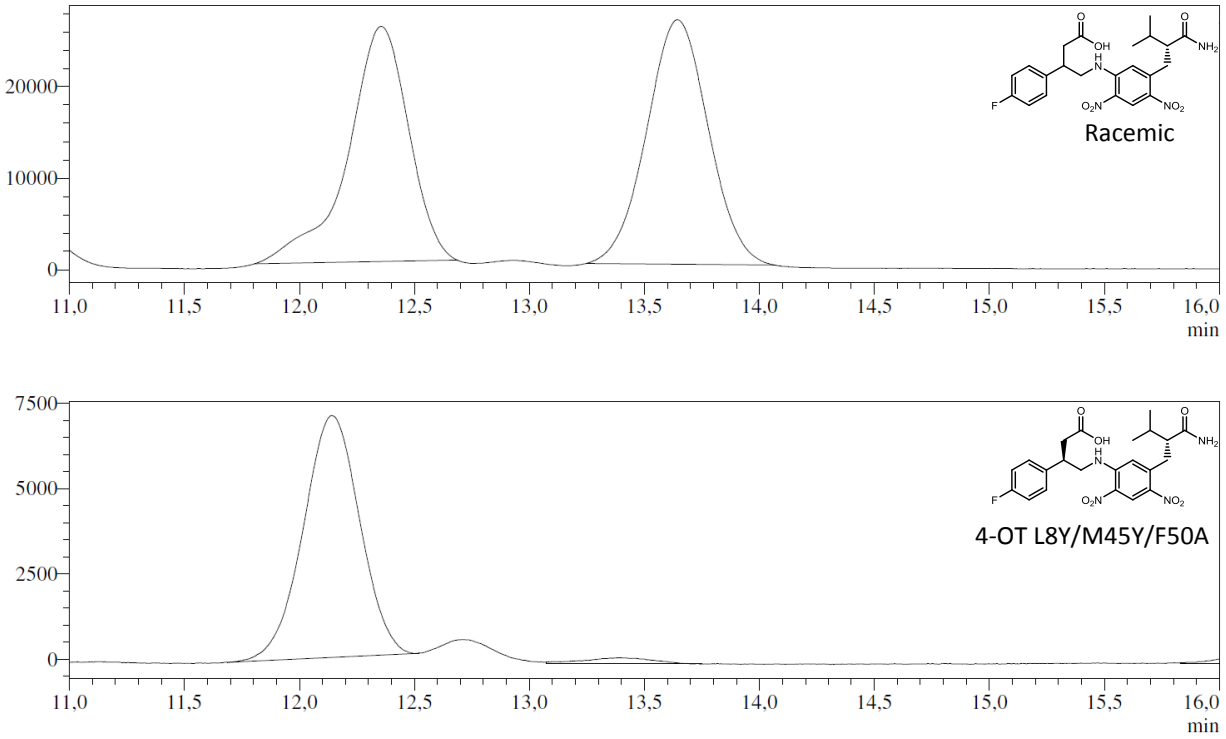

Figure S53. HPLC chromatograms of racemic and chemoenzymatically obtained derivatized **5d**.

References

1. van der Meer, J.; Poddar, H.; Baas, B.; Miao, Y.; Rahimi, M.; Kunzendorf, A.; van Merkerk, R.; Tepper, P. G.; Geertsema, E. M.; Thunnissen, A.M.W.H.; Quax, W.J.; Poelarends, G.J. Using Mutability Landscapes of a Promiscuous Tautomerase to Guide the Engineering of Enantioselective Michaelases. *Nat. Commun.* **2016***, 7,* 10911.

2. Zandvoort, E.; Baas, B.; Quax, W. J.; Poelarends, G. J. Systematic Screening for Catalytic Promiscuity in 4-Oxalocrotonate Tautomerase: Enamine Formation and Aldolase Activity. *ChemBioChem* **2011***, 12*, 602-609.

3. Waddell, W. J. A Simple Ultraviolet Spectrophotometric Method for the Determination of Protein. *J. Lab. Clin. Med.* **1956***, 48*, 311-314.

4. Geertsema, E. M.; Miao, Y.; Tepper, P. G.; de Haan, P.; Zandvoort, E.; Poelarends, G. J. Biocatalytic Michael-Type Additions of Acetaldehyde to Nitroolefins with the Proline-Based Enzyme 4-Oxalocrotonate Tautomerase Yielding Enantioenriched γ-Nitroaldehydes. *Chem. Eur. J.* **2013***, 19*, 14407-14410.

5. Kabsch, W. Integration, Scaling, Space-Group Assignment and Post-Refinement. *Acta Crystallogr., Sect. D* **2010***, 66*, 133-144.

6. McCoy, A. J.; Grosse-Kunstleve, R. W.; Adams, P. D.; Winn, M. D.; Storoni, L. C.; Read, R. J. Phaser Crystallographic Software. *J. Appl. Crystallogr.* **2007***, 40*, 658-674.

7. Poddar, H.; Rahimi, M.; Geertsema, E. M.; Thunnissen, A.M.W.H.; Poelarends, G. J. Evidence for the Formation of an Enamine Species During Aldol and Michael-type Addition Reactions Promiscuously Catalyzed by 4-Oxalocrotonate Tautomerase. *ChemBioChem* **2015***, 16*, 738-741.

8. Murshudov, G. N.; Vagin, A. A.; Dodson, E. J. Refinement of Macromolecular Structures by the Maximum-Likelihood Method. *Acta Crystallogr. , Sect. D* **1997***, 53*, 240-255.

9. Emsley, P.; Lohkamp, B.; Scott, W. G.; Cowtan, K. Features and Development of Coot. *Acta Crystallogr. , Sect. D: Biol. Crystallogr.* **2010***, 66*, 486-501.

10. Li, J.; Lear, M. J.; Kawamoto, Y. ; Umemiya, S.; Wong, A. R.; Kwon, E.; Sato, I.; Hayashi, Y. Oxidative Amidation of Nitroalkanes with Amine Nucleophiles Using Molecular Oxygen and Iodine. *Angew. Chem., Int. Ed.* **2015**, *127*, 13178-13182.

11. D'Oca, C. R. M.; Naciuk, F. F.; Silva, J. C.; Guedes, E. P.; Moro, C. C.; D'Oca, M. G. M.; Santos, L. S.; Natchigall, F. M.; Russowsky, D. New Multicomponent Reaction for the Direct Synthesis of β-Aryl-γ-nitroesters Promoted by Hydrotalcite-Derived Mixed Oxides as Heterogeneous Catalyst. *J. Braz. Chem. Soc.* **2017**, *28,* 285-298.

12. Zandvoort, E.; Geertsema, E. M.; Baas, B.; Quax, W. J.; Poelarends, G. J. Bridging Between Organocatalysis and Biocatalysis: Asymmetric Addition of Acetaldehyde to β-Nitrostyrenes Catalyzed by a Promiscuous Proline-Based Tautomerase. *Angew. Chem., Int. Ed.* **2012***, 124*, 1266-1269.

13. Szekrenyi, A.; Garrabou, X.; Parella, T.; Joglar, J.; Bujons, J.; Clapés, P. Asymmetric Assembly of Aldose Carbohydrates from Formaldehyde and Glycolaldehyde by Tandem Biocatalytic Aldol Reactions. *Nat. Chem.* **2015**, *7*, 724-729.

14. Jadhav, A.; Pathare, D.; Shingare, M. Validated Enantioselective LC Method, with Precolumn Derivatization with Marfey's Reagent, for Analysis of the Antiepileptic Drug Pregabalin in Bulk Drug Samples. *Chromatographia* **2007**, *65,* 253-256.